Ge^{73} Spin Relaxation Studies in Liquid Germanium Tetrafluoride

by

Marcelline Marie Tracey

A Dissertation Submitted in Partial Fulfillment
of the Requirements for the Degree of
Master of Science
in the Department
of
Chemistry
Simon Fraser University

APPROVAL

Name: Marcelline Marie Tracey

Degree: Master of Science

Title of Thesis: Ge^{73} Spin Relaxation Studies in Liquid Germanium Tetrafluoride

Examining Committee:

Dr. E. J. Wells
Senior Supervisor

J. M. D'Auria
Examining Committee

W. R. Richards
Examining Committee

E. M. Voigt
Examining Committee

Date Approved: 21 March 72

Abstract

Spin relaxation of spin-9/2 Ge^{73} in a pseudo-spherical environment is of interest because of the possibility of detecting relaxation pathways via higher order (magnetic octupole, electric hexadecapole) nuclear interactions.

Ge^{73} spin-lattice relaxation in liquid germanium tetrafluoride has been studied over the temperature range +31°C to -25°C by observation of the multiplet line widths of the scalar-coupled F^{19} spins in high resolution at 56.4 Mhz. The observed multiplet patterns at each temperature were decomposed by computer into a linear combination of the theoretical patterns arising from spin-9/2 relaxation due to fluctuating interactions involving spherical tensor spin operators of ranks zero, one, two, three, and four. Over the temperature range studied the relaxation pathway was found to be dominated by the rank-2 interaction, indicating a quadrupolar mechanism. No evidence was found for the third rank octupole or fourth rank hexadecapole mechanisms. Several processes were considered that could lead to fluctuating distortions from tetrahedral symmetry in the liquid phase: collisional distortion via London dispersion forces is proposed as the most likely. The measured activation energy of the relaxation process was $1.8 \pm .3$ kcal $mole^{-1}$.

Comparison of the present work with previously published data on GeH_4 indicates a misinterpretation of

that data in the literature, and leads to the conclusion that Ge^{73} spins in liquid GeH_4 relax via a first rank interaction, probably via competing mechanisms of spin-rotation interaction and intramolecular dipole-dipole coupling. The difference in mechanisms between the two systems can be understood by picturing GeH_4 as a 'hard-sphere' molecule and GeF_4 as a 'soft-sphere' molecule.

In liquid tetramethyl germanium, the smallness of the Ge^{73}-H^1 coupling constant ($3 \pm .2$ hz) prevented resolution of individual peaks of the proton decet from the strong centre band and from each other and precluded analysis.

Attempts to detect the F^{19} octet arising from spin-7/2, U^{235} in liquid UF_6 were unsuccessful on the A56/60 NMR spectrometer.

To Al

Table of Contents

List of Figures

List of Tables

Acknowledgements

Sincere thanks are extended by me to my research director, Professor E. J. Wells for the hours he spent helping me on this research project.

Thanks are also given to Dr. K. N. Slessor and R. Ferguson for their help with the computer programming.

Chapter I

Introduction

1. Spin relaxation

A charged nucleus that has a spin (i.e. any nucleus not having both mass and atomic number even) also has a magnetic dipole moment $\vec{\mu}_n$ which is parallel to, and proportional to the magnitude of the spin.

$$\vec{\mu}_n = \gamma_n \hbar \vec{I}$$

The $(2I + 1)$ allowable nuclear spin states of such a system are quantized, but are degenerate in the absence of an applied magnetic field. When the nucleus is placed in a strong magnetic field H, this degeneracy is lifted and the $(2I + 1)$ states become equally spaced, separated by $\gamma \hbar H$. At equilibrium, the levels will be populated according to a Boltzmann distribution.

In order to observe an effect in the NMR experiment, transitions must be induced between the energy states. One method is the application of an oscillating magnetic field at right angles to the strong magnetic field H. The oscillating magnetic field will cause transitions in both directions, i.e. induced emission and induced absorption. This would result in no net effect if the levels were equally populated. However, because of the Boltzmann effect, the levels have slight difference

in populations (Pople, Schneider, Bernstein, 1959), and thus NMR signals are detectable. However, continued application of the rf field would eventually equalize the populations, leading to a decreased signal intensity or no signal at all, unless the system has some way of re-establishing thermal equilibrium within itself. The process by which it does this is called relaxation, and, because this process involves energy exchange with the lattice, the process is known as spin-lattice relaxation. The time scale for this process is characterized by a spin-lattice relaxation time T_1.

In addition to the above, the nuclei also interact with one another. This spin-spin interaction (characterized by a time constant T_2) is a form of relaxation within the spin system and leads to broadening of the resonance line.

In considering T_1 and T_2, one must consider the entire sample (liquid in our case) by looking at the bulk magnetic moment $\vec{M}$ of a large ensemble of spins rather than at the individual spin wave functions and energy levels. In the absence of a field, a population difference n of the two energy levels (in a system in which $I = 1/2$) decays exponentially to equilibrium because of spin-lattice relaxation.

$$\frac{dn}{dt} = -\frac{n}{T} \tag{1}$$

Since M_z is proportional to n (Carrington, 1967)

$$\frac{dM_z}{dt} = -\frac{M_z}{T} \tag{2}$$

M_z is seen to decay to zero with some characteristic time T. Since there is no physical distinction between the direction z and the directions x and y in the absence of a field, both M_x and M_y decay to zero at the same rate as M_z.

However, once the sample is placed in a strong magnetic field aligned along some axis (usually designated as the z-axis), the situation changes. M_z no longer vanishes in thermal equilibrium but decays to a steady value M_o, where

$$M_o = \chi_o H_o \tag{3}$$

and

$$\chi_o = \frac{N\gamma^2\hbar^2 I(I+1)}{3kT} \tag{4}$$

T is the absolute temperature.
χ_o is the magnetic susceptibility and N is the number of spins. The decay of M_z now may often be approximated as

$$\frac{dM_z}{dt} = -\frac{(M_z - M_o)}{T_1} \tag{5}$$

in the case that T_1 is well defined.

Another difference is that although the components of M along the x and y directions, M_x and M_y, still decay exponentially to zero, they now do so in a time different from T_1. This new time is the transverse relaxation time, T_2. It is this value which determines the unsaturated line widths.

$$\frac{dM_x}{dt} = - \frac{M_x}{T_2} \qquad (6)$$

$$\frac{dM_y}{dt} = - \frac{M_y}{T_2}$$

T_1 and T_2 need not be equal since changes in M_x and M_y do not alter the total Zeeman energy of the nuclear spins, whereas changes of M_z need an exchange of Zeeman energy with the lattice (Carrington-2, 1967).

In an homogeneous field, the equation of motion of the nuclear magnetization for an ensemble of free spins can be shown (Abragam-1, 1961) to be

$$\frac{d\vec{M}}{dt} = \gamma(\vec{M} \times \vec{H}) \qquad (7)$$

If a small rf field, H_1, is now applied to the

system, the Bloch equations given above can be altered to account for the motion due to relaxation which is superposed on the motion of the free spins.

$$\frac{d\vec{M}}{dt} = \gamma(\vec{M} \times \vec{H}_o) + \gamma(\vec{M} \times \vec{H}_1) - \frac{(\vec{i}M_x + \vec{j}M_y)}{T_2} - \vec{k}\frac{(M_z - M_o)}{T_1} \tag{8}$$

where $\vec{H}_1 = H_1(\vec{i}\cos\omega t - \vec{j}\sin\omega t)$.

If we now transform to a new set of axes (x', y', z) which rotates with $\vec{H}_1$ at an angular frequency ω about the z-axis (Figure 1), equation 8 can be re-written in the rotating frame as (Abragam-2, 1961)

$$\frac{d\vec{M}}{dt} = \gamma(\vec{M} \times H_{eff}) - \frac{(iM'_x + jM'_y)}{T_2} - \vec{k}\frac{(M_z - M_o)}{T_1} \tag{9}$$

where M'_x and M'_y are the transverse components of M in the rotating frame. Separation of the three components of M then gives

$$\frac{dM'_x}{dt} = -\frac{M'_x}{T_2} + \Delta\omega M'_y$$

$$\frac{dM'_y}{dt} = -\Delta\omega M'_x + \gamma H_1 M_z - \frac{M'_y}{T_2} \tag{10}$$

Figure 1.

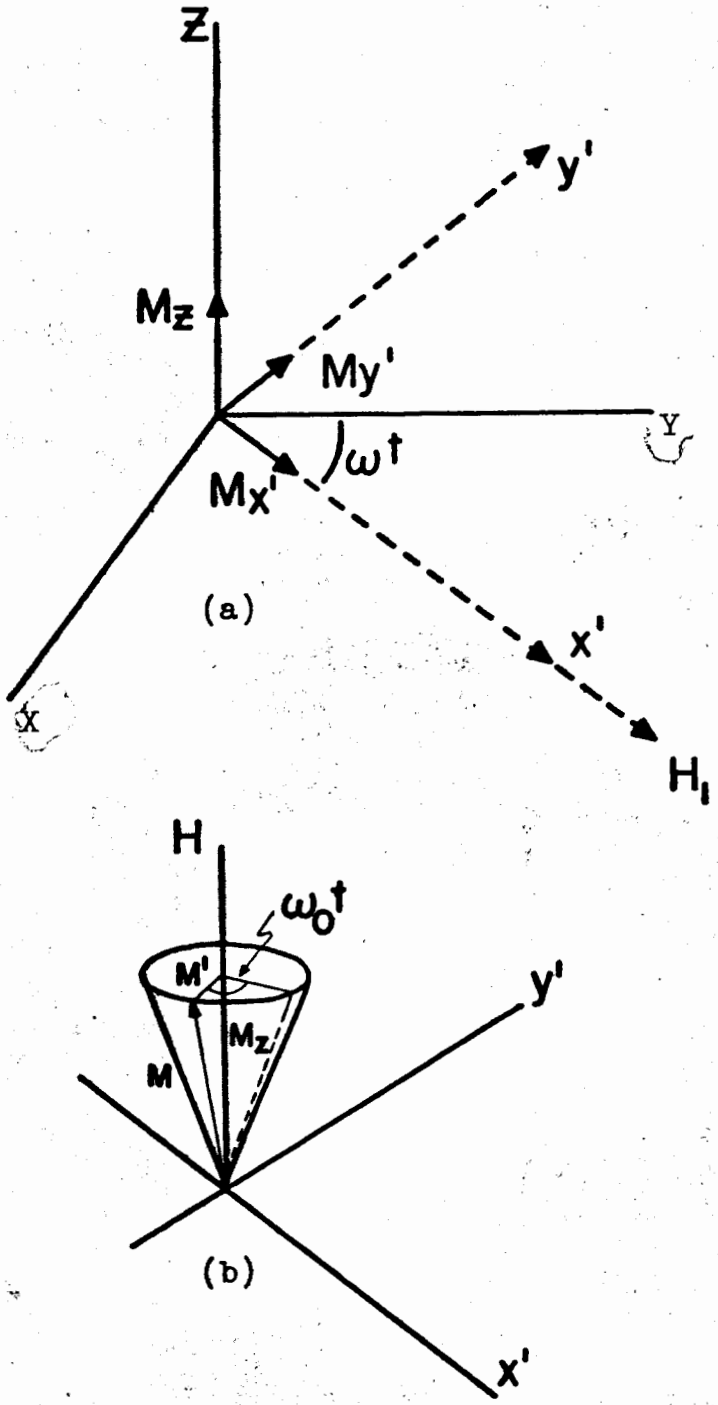

(a) The rotating coordinate system.

(b) Precession of nuclear magnetic moments about a steady magnetic field.

$$\frac{dM}{dt}_z = - \gamma_n H_1 M'_y - \frac{(M_z - M_o)}{T_1}$$

where $\Delta\omega = \omega_o - \omega$ and $\omega_o = -\gamma H_o$.

A steady state solution of equation 10 is found by setting

$$\frac{dM'}{dt}_x = \frac{dM'}{dt}_y = \frac{dM}{dt}_z = 0$$

If the rf field has been on for a sufficiently long enough time for the transient exponentials to decay, the steady state solutions of (10) can be written as

$$M'_x = \frac{\gamma H_1 T_2^2 \Delta\omega}{1 + T_2^2(\Delta\omega)^2 + \gamma^2 H_1^2 T_1 T_2} M_o$$

$$M'_y = \frac{\gamma H_1 T_2}{1 + T_2(\Delta\omega)^2 + \gamma^2 H_1^2 T_1 T_2} M_o \qquad (11)$$

$$M_z = \frac{1 + T_2^2(\Delta\omega)^2}{1 + T_2^2(\Delta\omega)^2 + \gamma^2 H_1^2 T_1 T_2} M_o$$

For negligible saturation, i.e. for $\gamma^2 H_1^2 T_1 T_2 \ll 1$, M'_y, which we shall call absorption, becomes

$$M'_y = \pi\gamma H_1 M_o f_{T_2}(\Delta\omega) \qquad (12)$$

where $f_{T_2}(\Delta\omega)$ is the normalized Lorentz shape function

$$f_{T_2}(\Delta\omega) = \frac{T_2}{\pi} \frac{1}{1 + (\Delta\omega)^2 T_2^2} \tag{13}$$

and has a half width at half intensity of $1/T_2$.

2. Literature Survey

Since the publication of the paper by Bloembergen, Purcell, and Pound (BPP, 1948), "Relaxation effects in Nuclear Magnetic Resonance Absorption", it has become a well-established fact that in NMR one has a convenient probe for studying molecular motion in liquids, since the nuclear spin relaxation time is related to molecular diffusion. Assuming rotational Brownian motion, BPP discussed the theory of dipole-dipole interaction, which is dependent on the magnitude and direction of the intra- and intermolecular vectors connecting the observed nuclear dipole with others in the liquid (Huntress, 1970). Shimizu (Shimizu, 1962) extended this theory to include dipolar effects resulting from Brownian motions which yield manifold correlation times rather than just one.

Spin-rotational interactions, arising from the interaction of a nuclear magnetic moment with the magnetic field produced at the nucleus by the rotation of the molecule, can prove to be an efficient method of relaxation in liquids. Rigny and Virlet (Rigny and Virlet, 1967) have estimated that in the case of liquid hexafluorides, this type of interaction can be responsible for at least 90% of the fluorine relaxation. Hubbard (Hubbard, 1963) outlined the theory for

this interaction also assuming the change in orientation of the molecule to be due to isotropic rotational Brownian motion. His theory was extended in 1968 (Huntress, 1968) to cover the effects of anisotropic molecular diffusion.

There is a drawback to each of the above mechanisms when it comes to using relaxation effects to describe molecular motion. In the case of dipolar relaxation, it is not always possible to separate the inter- from the intra-molecular contributions. For the spin-rotational case, both molecular reorientation and angular momentum changes are involved, and, often unseparable.

For a nucleus with spin I greater than 1/2, there is available one more mode of relaxation -- quadrupole relaxation, made possible through interaction of the quadrupole moment with the electric field gradient produced at the nucleus having the quadrupole moment. For a nucleus having a large quadrupole interaction, this mode of relaxation can prove to be an excellent method of describing molecular motion, especially if it swamps all other modes of relaxation, since the quadrupole interaction depends only on one motion -- molecular reorientation of the molecule arising from collisions or tumbling.

However, a quadrupole nucleus at a molecular site with zero static field gradient can still experience quadrupolar relaxation. This mechanism was first discussed by Staub and co-workers (Staub, 1954), who noted a relaxation mechanism arising from a strong collisional electric interaction in gaseous Xe in their communication on the nuclear magnetic moments of Xe^{129} and Xe^{131}, and invoked it to explain the disparity in relaxation times of Xe^{131} ($I = 3/2$) and Xe^{129} ($I = 1/2$). This mechanism wss identified clearly as a quadrupole effect in a paper by Staub (Staub, 1956) in which he discusses the possibility of the strong Van der Waals forces in the Xe gas deforming the electron shell to produce an inhomogeneous electric field at the nucleus.

A theoretical discussion of the above interaction was first published by Casimir (Casimir, 1936) and this theory applied to a crystal structure by Pound (1950).

However, in a molecular substance, there usually is the possibility of more than one form of relaxation mechanism within the spin system, thus affording a relaxation rate that is actually a sum of rates. An attempt to separate the different contributions to the relaxation time was made by Bloom (Bloom, 1962; 1969) and by Ozier and his fellow workers (Ozier, 1968), so

that the temperature dependence of each could be tested separately and applied to a chemical system.

A novel approach to relaxation rates was used by Brooks in his work (S. Brooks, 1969) on heavy metal hexafluorides and also was noted by Dreeskamp (1966). In much the same way as Bloom tried to separate the contributions to the overall T_1 of the system, this approach assigned line widths contributions not only to specific relaxation processes but also attempted to assign portions of the line widths as arising from relaxations of only part of the molecule, in this case, the heavy metal ion.

3. Present Project

Following the method of S. Brooks, we examine the relaxation mechanisms of the Ge^{73} nucleus in the GeF_4 molecule in the liquid phase. The technique is an indirect one, utilising the intramolecular scalar coupling between the insensitive, low-γ, low abundance Ge^{73} spins and the abundant, sensitive F^{19} spins. Thus the scalar J-coupling acts as a nuclear amplifier, with the additional advantage that in the easy-to-observe F^{19} spectrum the individual components of the coupled decet monitor uniquely the M to M' relaxation transitions among the $(2I + 1)$ Zeeman states of Ge^{73}. This M-dependence is lost in a direct T_1 measurement owing to the degeneracy of the M to M + 1 transition frequency, but we show that the M dependence of the relaxation contains important information on the relaxation mechanism. We point out that in addition to a loss of information, the direct method in this case would be accompanied by severe experimental difficulties caused by adverse signal-to-noise ratio associated with direct observation of the Ge^{73} resonance.

On the theoretical side, we develop what we believe to be a novel classification of relaxation mechanisms based on the tensor rank of the spin operator involved in the spin-lattice interaction. Although this concept was

implicit in Brooks' thesis, it is here made explicit, and the relationship to the observed spectral patterns is clarified.

The analysis of the spectral patterns observed in the F^{19} multiplet is straightforward. In the limit of slow transverse relaxation ($R_{2_F} << 2\pi J_{Ge-F}$, which turns out to be the case here) each member of the 10-line F^{19} decet has a linewidth small compared to the multiplet splitting, and a Lorentzian lineshape. Since each component of the multiplet has the same integrated area (to within a few ppm due to the Boltzmann factor) and the same lineshape, the multiplet linewidths (which can only be measured inaccurately) are inversely proportional to the multiplet peak heights (which can be more accurately determined). Then the measurement of one or two peak widths and a set of relative peak heights leads to a set of accurate linewidths at each temperature. These experimental linewidths $\Delta\nu_{1/2}$ (M) vary from component to component in the multiplet and yield the M-dependent F^{19} transverse relaxation rates:

$$R_{2,F}(M) = 1/T_{2,F}(M) = \pi\Delta\nu_{1/2}(M)$$

Each $R_{2,F}(M)$ is, in its turn, the sum of purely transverse effects on the F^{19} spins (inhomogeneity broadening R_2^*,

exchange broadening $R_{2,exch}$, and natural F^{19} dephasing $R_{1,F}$ -- independent of M(Ge)) and J-transmitted uncertainty-broadening due to longitudinal, M-dependent $R_{1,Ge}(M)$ effects, i.e.

$$R_{2,F}(M) = R_2^* + R_{2,exch,F} + R_{1,F} + R_{1,Ge}(M)$$

The Ge^{73} relaxation may in principle be due to a sum of competing interactions of ranks Ω varying from 1 to 4 with weights $a^{(\Omega)}$ and M-dependent coefficients $\lambda(\Omega)$ obtained from the squares of the appropriate Clebsch-Gordon coefficients. The M-independent terms due solely to the F^{19} behaviour can be included as a zero rank contribution, so we can write finally

$$R_{2,F}(M) = \sum_{\Omega=0}^{4} a^{(\Omega)} \lambda_M^{(\Omega)}$$

Thus the problem resolves itself into a linear decomposition of the observed pattern at each temperature into a sum of calculable contributing patterns, where the five independent $a^{(\Omega)}$'s are to be determined. Since the decet is symmetric in $\pm$ M, each pattern is characterized by five experimental line-widths, yielding a set of five equations in the five unknown $a^{(\Omega)}$. Actually, the equations are over-determined by one, since

the value of $a^{(o)}$ due to F^{19} processes alone can be independently obtained from the line-width of the strong central F^{19} resonance, due to molecules where the fluorine nuclei are bonded to non-magnetic Ge isotopes. Hence a unique pattern decomposition should be possible at each temperature, and it should be possible to obtain the temperature dependence of every contributing mechanism via the $a^{(\Omega)}(T)$'s.

The Ge^{73} spin system in GeF_4 is of interest on several counts:

a) $Ge^{73}F_4$ represents one of a relatively few neutral molecular species containing a quadrupolar nucleus in a highly symmetric environment. Other members of this class include $Mo^{95,97}F_6$ (studied by Brooks in 1969); $S^{33}F_6$ (limited by the low natural abundance of S^{33} (0.76%)); $Ge^{73}H_4$, studied by Sackmann and Dresskamp (1966); $Ge^{73}(CH_3)_4$ and $U^{235}F_6$, which are both examined here.

b) The magnetic dipole moment of Ge^{73} is very small, Table VI, reducing the cross-section for first rank magnetic dipole relaxation transitions.

c) The high tetrahedral symmetry of the molecule reduces the static (averaged) electric field gradient at the Ge^{73} nucleus to zero. This implies that the cross-section for second-rank electric quadrupole relaxation

should be zero to first order.

d) The possibility then exists that the dominant Ge^{73} relaxation may be non-vanishing higher-order nuclear interactions (magnetic octupole, electric hexadecapole). These interactions are generally taken to be negligible, and have never been shown to contribute appreciably to any nuclear relaxation. Since the correlation time governing the fluctuation of these interactions is different to those of the normal first and second rank interactions, their measurement would yield another parameter in the description of overall molecular motion in the liquid.

Chapter 2

Theory

1. Relaxation mechanisms in liquids

Nuclear relaxation processes in liquids are related to the molecular thermal motions within the liquid samples. The fluctuating megnetic field due to these rapid molecular motions are characterized by moderate amplitudes and randomness; the motions include rotational tumbling of individual molecules, relative translational motion of molecules, and chemical exchange (Abragam-3, 1961). We need some way to measure the strength and frequency distribution of the resulting nuclear magnetic interactions.

Let the random interaction be defined by a function f(t) which fluctuates around the mean value of zero. The frequency spectrum is obtained by taking the Fourier transform of this function over some time interval -T to +T.

$$f(\omega) = \int_{-\tau}^{\tau} f(t) e^{i\omega t} dt \qquad (14)$$

The new function is also a random function which varies from sample to sample. It's square $|f(\omega)|^2$ has a definite average value.

We can now define a new function $G(\tau)$.

$$G(\tau) = \overline{f^*(t+\tau) f(t)} \qquad (15)$$

which is called the correlation function. It correlates the random function at some time t with its value at some other time t + τ (Carrington-3, 1967). This function has a large value for short times and goes to zero as τ increases. If G(τ) drops off exponentially to zero with a decay time τ_c, equation 15 will then look like

$$G(\tau) = \overline{f^*(t)f(t)e^{|\tau|/\tau_c}} \qquad (16)$$

where τ_c is called the correlation time and can be thought of as the memory time of the system. The power spectrum or spectral density of f(t) is then the Fourier transform of the correlation function.

$$J(\omega) = \int_{-\infty}^{\infty} G(\tau)e^{i\omega\tau}\,d\tau \qquad (17)$$

This becomes, for exponential decay as in equation 16,

$$J(\omega) = \frac{2\tau_c}{1 + \omega^2\tau_c^2}\,\overline{f^*(t)f(t)} \qquad (18)$$

In NMR relaxation studies, the random fields of interest are those which induce transitions between the energy levels of the individual spins or spin

system, and thus broaden the Zeeman lines. The transition probability for such a process is given by (Abragam-4, 1961)

$$W_{MM'} = \int_{-t}^{t} \overline{\langle M' | \mathcal{H}_1(t_1) | M \rangle \langle M | \mathcal{H}_1(t) | M \rangle} \, e^{i\omega\tau} \, dt_1 \quad (19)$$

where $\mathcal{H} = \mathcal{H}/\hbar$ rad sec^{-1}. However, since $\mathcal{H}_1(t)$ is taken to be a random function, the quantity under the bar, corresponding to equation 15, is just the correlation function of $\langle M' | \mathcal{H}_1(t) | M \rangle$. The transition probability then has the form

$$W_{MM'} = \int_{-t}^{t} G_{MM'}(\tau) e^{i\omega\tau} \, d\tau \quad (20)$$

where $\tau = t - t_1$. Following usual procedure in time-dependent perturbation theory, $|t|$ is allowed to increase infinitely and, using equations 19 and 17,

$$W_{MM'} = J(\omega) \quad (21)$$

$$= \frac{2\tau_c}{1 + \omega^2 \tau_c^2} \overline{\langle M' | \mathcal{H}_1(t) | M \rangle}^2 \quad (22)$$

for an exponential correlation function.

The correlation time, τ_c, is the time taken for a typical fluctuation to decay to 1/e of its amplitude. In the extreme narrowing case (Abragam-5) $\omega\tau_c \ll 1$, and equation 22 becomes

$$W_{MM'} = 2\tau_c \overline{\langle M' | \mathcal{H}_1(t) | M \rangle}^2 \qquad (23)$$

Table I lists the possible ways in which $\mathcal{H}_1(t)$ can be generated and the correlation times that can be attributed to the processes.

The theory for molecular reorientation in the liquid is presently unsatisfactory, but if the model we choose to use for the liquid GeF_4 is the Debye rotational-diffusion model, the molecule is pictured as a small sphere of radius a embedded in a viscous fluid of viscosity η. The diffusion constant for rotation D, is given by Stoke's Formula

$$D = \frac{kT}{8\pi a\eta}$$

Furthermore, the correlation time is related to the diffusion constant by the formula (Abragam-6)

$$\frac{D}{a^2}\, \iota(\iota + 1) = \frac{1}{\tau_\iota}$$

Table I

Spin Relaxation Mechanisms

Mechanism	$\mathcal{H}_1(t)$	Spin Operator		Correlation Times
Dipole-dipole	$\vec{I}\cdot\underset{\approx}{\mathcal{D}}(t)\cdot\vec{S}$	$T^{(2)}(I,I)$ $T^{(1)}(I)$	$I=S$ $I\neq S$	τ_2 (intramolecular) τ_1 (intermolecular)
Quadrupolar	$\vec{I}\cdot\underset{\approx}{\mathcal{A}}(t)\cdot\vec{I}$	$T^{(2)}(I,I)$	$I>\frac{1}{2}$	τ_2 (intramolecular) $\tau_{\text{collisional}}$ (collisional)
Scalar	$\vec{I}\cdot\underset{\approx}{\mathcal{A}}(t)\cdot\vec{S}(t)$	$T^{(1)}(I)$	$S\neq 0$	$T_1(S)$ or τ_2 of $\mathcal{A}(t)$
Spin-rotation	$\vec{I}\cdot\underset{\approx}{\mathcal{L}}(t)\cdot\vec{J}(t)$	$T^{(1)}(I)$		τ_2 of $\mathcal{L}(t)$ τ_J of $\vec{J}(t)$
Anisotropic Shift	$\vec{I}\cdot\underset{\approx}{\sigma}(t)\cdot H_0\vec{k}$	$T^{(1)}(I)$		τ_2 of $\sigma(t)$
Plus possible higher order interactions:				
Octupole	$\vec{I}\cdot\underset{\approx\approx}{\mathcal{O}}(t):\vec{I}\vec{I}$	$T^{(3)}(I)$	$I>1$	τ_3 of $\mathcal{O}(t)$
Hexadecapole	$\vec{I}\vec{I}:\underset{\approx\approx}{\eta}(t):\vec{I}\vec{I}$	$T^{(4)}(I)$	$I>3/2$	τ_4 of $\eta(t)$

For NMR studies, $\iota = 2$, and

$$D = \frac{a^2}{6\tau_2}$$

Therefore,

$$\tau_2 = \frac{4\pi\eta a^3}{3kT} \qquad (24)$$

Equation 24 is valid only for spheres much greater than molecular size since the viscosity η is a macroscopic quantity. Equation 24 is also only valid for $\omega\tau_2 \ll 1$ (Abragam-7).

The correlation times τ_2 and τ_J need not be the same since they arise from different motions of the molecule; τ_2 arising from molecular reorientation, and τ_J from angular momentum changes due to collisions. They are however related by the formula (Hubbard, 1963)

$$\tau_J\tau_2 = \frac{I}{6kT}$$

Hubbard also writes that, although the angular momentum and the orientation of a molecule are not independent, if the motion of the molecules is such that the components of the angular momentum change much more rapidly than the

rotation functions $\mathfrak{D}_{M,M'}(\Omega)^{\dagger}$ of the orientation, or vice versa, one would expect the time dependence of the correlation function to be determined by the more rapidly fluctuating function.

†The functions mentioned in Hubbard's paper (Hubbard, 1963) are the rotation matrix operators discussed by Edmonds (Edmonds, 1957, Chapter 4) for transforming from one frame of reference to another. The symbol Ω represents the three Euler angles α, β, γ.

2. Tensor notation.

If the scalar interaction energy of two parts of any quantum mechanical system is invariant under arbitrary rotations of the space-fixed axes, then the energy can be written most generally as a scalar contraction of two irreducible spherical tensors (Edmonds, 1957). Often, the system may be divided into two distinct parts, each part being characterized by some angular momenta, so that one tensor depends exclusively on one set of variables and the other tensor on a set of variables in a different space. (In our case, the two parts are the spin system and the lattice system.). The reduced matrix element, which contains the M-dependent matrix we are interested in, may be determined using the Wigner-Eckart theorem

$$\langle I,M'|T^{\iota}_{\mu}|I,M\rangle = (-1)^{I-M}\begin{pmatrix} I & I & \iota \\ -M & M' & \mu \end{pmatrix}\langle I\|T^{\iota}\|I\rangle \quad (25)$$

if any one of the matrix elements of an irreducible set of spherical tensors T^{ι}_{μ} of rank ι is known in the I,M representation (Benz, 1966). The symbol in parenthesis is the Wigner 3-j symbol and it carries all the M-dependence for the interaction. It is a symmetrized Clebsch-Gordon coefficient, which is given,

in Rose's notation (Rose, 1957) by Edmonds (1957).

$$\begin{pmatrix} j_1 & j_2 & j_3 \\ m_1 & m_2 & m_3 \end{pmatrix} = (-1)^{j_1-j_2-m_3}(2j_2+1)^{-\frac{1}{2}}C(j_1j_2j_3;m_1m_2-m_3) \quad (26)$$

Moreover, for the particular case in which we are interested (relaxation of a single nuclear spin I in the nuclear ground state) the I dependence is trivial, is carried by the so-called "reduced matrix element" $\langle I\| T^t \| I\rangle$ and simply weights each rank t of interaction through the spin tensor operator T^t.

Then the mechanisms leading to nuclear spin relaxation of a single spin I are readily classified according to the rank t of the resulting spin operators, as is done below. And since each rank operator on a given spin I implies a unique M-dependence through the Clebsch-Gordon coefficient in (26), we see that an experimental determination of the M-dependence is then sufficient to decompose a relaxation into its contributing mechansims. This is the crux of the approach taken in this thesis, and to our knowledge represents a novel attack on the unravelling of spin relaxation mechanisms. As a convenient monitor of the M-dependence of the mechanism we use the line-widths of each member of a scalar-coupled spin multiplet in high resolution NMR; and as a

bonus advantage, we can then obtain the increased sensitivity of a set of high-γ spins-$\frac{1}{2}$ coupled to a low γ spin $I > \frac{1}{2}$ of interest.

As part of a systematic study of relaxation mechanisms of high-Z nuclear spins in the liquid phase, the system chosen here is neat liquid germanium tetrafluoride, where the nuclear spin of interest is 7% abundant $I = 9/2$ Ge^{73}. This system was regarded as of some importance because:

a) the molecular structure has been shown to be (Appendix, P. 93) tetrahedral, so that the static electric field gradient at the Ge^{73} nucleus vanishes, and thus the first order nuclear quadrupole interaction vanishes.

b) the relatively high value of the nuclear spin (9/2) allows the definite possibility of relaxation mechanisns vis higher order electric and magnetic interactions (magnetic octupole, electric hexadecapole, etc.) which are not forbidden by molecular symmetry. These possible mechanisms have not yet been shown to be operative in any system.

c) The directly bonded and scalar-coupled $F^{19}(I=1/2)$ spins afford a convenient and sensitive test of processes occurring at the Ge^{73} site.

Rank Classification of Relaxation Mechanisms

We now investigate the various possible mechanisms occurring at a spin $I > \frac{1}{2}$ as viewed from the line-widths of one or more symmetrically equivalent scalar-coupled spin-$\frac{1}{2}$ nuclei in high resolution. We can classify possible mechanisms according to their rank, but the tensor operator theory is ambiguous to mechanisms of a given rank. To classify mechanisms within a given rank, it will generally be necessary to either obtain more information, such as the temperature dependence of the experimental relaxation rates, or to apply one's intuition as to the dominant mechanism applying within that rank.

The possible mechanisms can be systematized in the following manner:

a) Zero rank tensor $T^{(0)}$. The transition probability (equation 22) is independent of the M-state of Ge^{73}. The zero rank tensor could be manifested by such things as ΔH_0 inhomogeneity effects, F^{19} T_1 effects, and F^{19} chemical exchange effects.

b) First rank tensor. This rank tensor operator on spin I includes the following possible relaxation mechanisms:

Spin rotation $\vec{I}.\underset{\approx}{C}.\vec{J}$ $\quad \sum_{\mu} (-1)^{\mu} T_{\mu}^{(1)}(C,J)\ T_{-\mu}^{(1)}(I)$

Heteronuclear dipole $\vec{I}.\underset{\approx}{D}.\vec{S}$ $\quad \sum_{\mu} (-1)^{\mu} T_{\mu}^{(1)}(D,S)\ T_{-\mu}^{(1)}(I)$

Scalar relaxation $\vec{I}.\underset{\approx}{A}.\vec{S}$ $\quad \sum_{\mu} (-1)^{\mu} T_{\mu}^{(1)}(A,S)\ T_{-\mu}^{(1)}(I)$

c) Second rank tensor.

Quadrupole effect. $\vec{I}.\underset{\approx}{A}.\vec{I} \sum_{\mu} (-1)^{\mu} T_{\mu}^{(2)}(A)\, T_{-\mu}^{(2)}(I,I)$

d) Third rank tensor.

Octupole effect $\vec{I}.\underset{\approx\approx}{A}:\vec{I}\vec{I} \sum_{\mu} (-1)^{\mu} T_{\mu}^{(3)}(A)\, T_{-\mu}^{(3)}(I,I,I)$

e) Fourth rank tensor $T^{(4)}(I,I,I,I)$.

Hexadecapole effect.

Then to obtain the theoretical spectrum for a given rank interaction, one writes the theory for each of the mechanisms until it is in the form given above and then uses the Wigner-Eckart theorem. This is done in the following section for those mechanisms pertinent to our system (Ge^{73}, $I = 9/2$).

3. Dipolar Interaction

The dipole-dipole relaxation mechanism depends upon the interaction of one nuclear magnetic dipole with another. The energy of the interaction is dependent on the magnitude and direction of the intra- and intermolecular vectors connecting the observed dipole with the others in the liquid, these vectors being changed by molecular motions in the liquid (Huntress, 1968; 1970).

The classical expression for the interaction energy E between two magnetic moments $\vec{\mu}_I$ and $\vec{\mu}_S$ is

$$E = \frac{\vec{\mu}_I \cdot \vec{\mu}_S}{r^3} - \frac{3(\vec{\mu}_I \cdot \vec{r})(\vec{\mu}_S \cdot \vec{r})}{r^3} \qquad (27)$$

where $\vec{r}$ is the radius vector between the two moments. To change to the quantum mechanical case, the following substitution is made.

$$\vec{\mu}_I = \gamma_I \hbar \vec{I}$$

$$\vec{\mu}_S = \gamma_S \hbar \vec{S}$$

with the vectors being separated by

$$\vec{r} = (r_{IS}, \theta_{IS}, \varphi_{IS})$$

The interaction Hamiltonian then becomes

$$\mathcal{H}_{dip} = \gamma_I \gamma_S \left[\frac{(\vec{I} \cdot \vec{S})}{r^3} - \frac{3(\vec{I} \cdot \vec{r})(\vec{S} \cdot \vec{r})}{r^3} \right] \quad (28)$$

When the term in brackets is multiplied out, it can be shown (BPP, Tinkham, 1964) that the dipolar Hamiltonian can be put in the form of second rank tensors. Following the tensor notation, then, equation 28 has the form (Bloom, 1969).

$$\mathcal{H}_{dip} = n\left(\frac{24\pi}{5}\right)^{\frac{1}{2}} \frac{\gamma_I \gamma_S}{r^3} \sum_{\mu=-2}^{+2} (-1)^{\mu} T_{\mu}^{(2)}(I,S) Y_{2,-\mu}(\theta,\varphi) \quad (29)$$

where n is the number of equivalent S spins.

Using the extreme narrowing limit of equation 22, i.e. the case where

$$W = 2\tau_c \overline{\langle I,M' | \mathcal{H} | I,M \rangle}^2$$

and substituting equation 29, the probability of induced transitions among the M-states of our system by dipolar interaction is given by

$$W = n\,2\tau_c \frac{24\pi}{5} \frac{1}{4\pi} \frac{\gamma_I^2 \gamma_S^2 \hbar^2}{r^6} \left| \langle I,M' | \sum_{\mu=-2}^{+2} T_{\mu}^{(2)}(I,S) | I,M \rangle \right|^2 \quad (30)$$

noting that for an isotropic medium

$$\langle Y_{2,\mu}(\theta,\varphi)\rangle^2 = \frac{1}{4\pi}$$

If we can assume that the two spins I and S are relaxing independently, then we can use the expression for the spherical tensor $T_\mu^{(2)}(I,S)$ as given by Rose (Rose-2, 1957).

$$T_\mu^{(2)}(I,S) = \sum_{\mu=-1}^{+1} C(112;\mu_1, \mu-\mu_1) T_{\mu_1}^{(1)}(I) T_{\mu-\mu_1}^{(1)}(S) \quad (31)$$

$C(112;\ 0\ 0) = (2/3)^{\frac{1}{2}}$; $C(112;\ 1\ -1) = C(112;\ -1\ 1) = (1/2)^{\frac{1}{2}}$

$T_0^1(I) = I_z$

$T_{\pm 1}^1(I) = \mp 2^{-\frac{1}{2}} I_{\pm} = \mp 2^{-\frac{1}{2}}(I_x \mp iI_y)$

For heteronuclear dipolar relaxation of spin I, the selection rules from $T_\mu^{(1)}(I)$ in equation 31 show that $\Delta M = \pm 1$.

Applying equation 31 to equation 30, we get:

$$W = \frac{6}{5} n\tau_c \frac{\gamma_I^2\gamma_S^2\hbar^2}{r^6} S(S+1) \langle I,M'| T_{\pm 1}^{(1)}(I) |I,M\rangle \quad (32)$$

The Wigner-Eckart theorem (equation 25) can now be applied to give

$$W = A_{dip} S(S+1) \begin{pmatrix} I & I & 1 \\ -M & M' & \mu \end{pmatrix}^2 (I\| T^{(1)} \| I)^2 \quad (33)$$

4. Spin rotation interactions

Interaction of a nuclear magnetic moment with the magnetic field produced at the position of the nucleus by the rotation of the molecule containing the nucleus is called a spin-rotational interaction. This type of interaction has been shown (Hubbard, 1963; Huntress, 1968; Rigny and Virlet, 1967) to be of importance when considering nuclear magnetic relaxation of liquids.

If the molecule rotates at an angular velocity $\vec{\omega}$, the angular momentum is

$$I\vec{\omega} = \vec{J}\hbar$$

where I is the moment of inertia of the molecule. If the rotation is free, as in a dilute gas, J is the angular momentum operator and is quantized with eigenvalues J = 0, 1, 2, ... However, in a liquid J may no longer be a good quantum number since intermolecular interactions may restrict free rotation (Green and Powles, 1965). (I.e. The molecule will undergo frequent collisions and J will become a function of time.).

From equation 22, the transition probability between two states M and M' due to some fluctuating Hamiltonian is

$$W_{MM'} = \overline{\langle M' | \mathcal{H}_1(t) | M \rangle}^2 \frac{2\tau_c}{1 + \omega^2\tau_c^2}$$

For spin-rotation interaction, the fluctuating Hamiltonian has the form

$$\mathcal{H}_{sr} = \vec{I}.\underset{\approx}{c}(t).\vec{J}(t) \qquad (34)$$

where $\underset{\approx}{c}$ is the spin-rotation interaction tensor, $\vec{I}$ is the nuclear spin angular momentum; and $\vec{J}$ is the rotational angular momentum. For a nucleus at the centre of a spherically symmetrical molecule, c has the form of a scalar, and it is J which carries the time dependence of the Hamiltonian. Equation 34 then becomes

$$\mathcal{H}_{sr} = c\vec{I}.\vec{J}(t)$$

The random function now has the form

$$\overline{\langle M'|\mathcal{H}_{sr}|M\rangle}^2 = c_{sr}^2 \overline{|\langle M'|\vec{I}.\vec{J}(t)|M\rangle|}^2$$

However, J(t) can be considered part of the lattice system since it causes no change in the spin system. Therefore, the above equation will read

$$\overline{\langle M'|\mathcal{H}_{sr}|M\rangle}^2 = c_{sr}^2 \langle J\rangle_{av}^2 \overline{\langle M'|\vec{I}|M\rangle}^2 \qquad (35)$$

since the only effects we are interested in are those causing transitions among the M-states of our system.

Since the $\vec{I}$ vector operators transform as irreducible tensors of rank one (Rose-3, 1957), the matrix elements of equation 35 can as before be obtained by use of the Wigner-Eckart theorem.

$$\langle I,M'|T^{(1)}_{\mu}|I,M\rangle = (-1)^{I-M'}\begin{pmatrix} I & I & 1 \\ -M & M' & \mu \end{pmatrix} (I\|T^{(1)}\|I) \qquad (36)$$

5. Nuclear Quadrupole Interactions

The electrostatic interaction energy between a nuclear charge distribution $\rho_N(r_N)d\tau_N$ and an electron charge distribution $\rho_E(r_E)d\tau_E$ can be written (Matthias, 1962; Abragam-8; Mahler, 1966)

$$E_{el} = \iint_N \iint_E \frac{\rho_N \rho_E \, d\tau_N \, d\tau_E}{|\vec{r}_N - \vec{r}_E|} \tag{37}$$

If we assume that there is no penetration by the electron into the nucleus, $\vec{r}_E > \vec{r}_N$, and the term $1/|\vec{r}_N - \vec{r}_E|$ can be expanded to give

$$\frac{1}{(\vec{r}_N - \vec{r}_E)} = \sum_l \frac{r_N^l}{r_E^{l+1}} P_l(\cos \omega_{EN}) \tag{38}$$

where $\cos \omega_{EN}$ is the angle between the directions of $\vec{r}_E$ and $\vec{r}_N$. Using the addition theorem of spherical harmonics (Edmonds, 1957)

$$E_{el} = \sum_{l=0}^{\infty} \frac{r_N^l}{r_E^{l+1}} \frac{4\pi}{2l+1} \sum_{\mu=-l}^{l} (-1)^\mu Y^l{}_\mu(\theta_E, \varphi_E) Y^l_\mu(\theta_N, \varphi_N) \quad x$$

$$\rho_N \rho_E \, d\tau_N \, d\tau_E \tag{39}$$

By introducing tensor operators, we can write the interaction Hamiltonian in the form

$$\mathcal{H}_{el} = \sum_{i=0}^{\infty} \sum_{\mu=-i}^{i} (-1)^{\mu} T_{\mu}^{i} \; V_{-\mu}^{i} \qquad (40)$$

where T_{μ}^{i} is the tensor operator of the nuclear moments and has the form

$$T_{\mu}^{i} = \left(\frac{4\pi}{2i+1}\right)^{\frac{1}{2}} \rho_N \, r_N^{i} Y_{\mu}^{i}(\theta_N, \varphi_N) \, d\tau_N$$

$V_{-\mu}^{i}$ is the tensor operator of the field and has the form

$$V_{-\mu} = \left(\frac{4\pi}{2i+1}\right)^{\frac{1}{2}} \rho_E \frac{1}{r^{i+1}} \, Y_{-\mu}^{i}(\theta_E, \varphi_E) \, d\tau_E$$

The first term in equation 40, $ZeV^{(o)}(0)$, Ze being the total charge, represents the electrostatic energy of a point nucleus. Since it is independent of nuclear size, shape or orientation, it will shift all magnetic levels equally, if there is any effect at all. Therefore, it tells us nothing about the nucleus as far as this work goes. The second term, with $i = 1$, is the electric dipole term and it vanishes due to conservation of parity (Abragam-9; Rose-4, 1957). For this reason, all electric interactions of odd i will vanish.

The first term of interest is then the $i = 2$ term. The electric interaction Hamiltonian for the quadrupole case is then

$$\mathcal{H}_{el} = \frac{4\pi}{5} \sum_{\mu=-2}^{2} (-1)^{\mu} T_{\mu}^{(2)} V_{-\mu}^{(2)}$$

The quadrupole interaction matrix elements are then given by (Matthias et al, 1962)

$$\langle I,M' | \mathcal{H}_{el} | I,M \rangle = \frac{4\pi}{5} \sum_{\mu=-2}^{2} (-1)^{\mu} \langle I,M' | T_{\mu}^{(2)} | I,M \rangle V_{-\mu}^{(2)} \quad (41)$$

Following Edmonds treatment (Edmonds-2, 1957) of the Wigner-Eckart theorem,

$$\langle I,M' | \mathcal{H}_{el} | I,M \rangle = \frac{4\pi}{5} \sum_{\mu=-2}^{2} (-1)^{\mu+I-M} \begin{pmatrix} I & I & 2 \\ -M & M' & \mu \end{pmatrix} (I \| T^{(2)} \| I) V^{(2)} \quad (42)$$

From selection rules, $-M + \mu + M' = 0$, so that there is only one μ for any given values M and M'. This means the summation over μ can be dropped.

The electric quadrupole moment eQ of the nucleus is defined as

$$eQ = \langle II | \sum_N e_N (3z_N^2 - r_N^2) | II \rangle$$

From the expression for the tensor operator of the nuclear moments given above,

$$T_0 = \left(\frac{4\pi}{5}\right)^{\frac{1}{2}} \sum_N e_N r_N^2 Y_0^{(2)}(\theta_N, \varphi_N)$$

From tables on Y_μ^1 :

$$T_o = \left(\frac{4\pi}{5}\right)^{\frac{1}{2}} \sum_N e_N r_N^2 \frac{1}{4} \left(\frac{5}{\pi}\right)^{\frac{1}{2}} (3\cos^2\theta_N - 1)$$

$$= \left(\frac{4\pi}{5}\right)^{\frac{1}{2}} \sum_N e_N \frac{1}{4} \left(\frac{5}{\pi}\right)^{\frac{1}{2}} (3z_N^2 - r_N^2)$$

The electric quadrupole moment is then given by

$$eQ = 2\langle II| T_0^{(2)}| II\rangle$$

Applying the Wigner-Eckart theorem to this equation, we obtain

$$eQ = 2\begin{pmatrix} I & I & 2 \\ -I & I & 0 \end{pmatrix} (I\| T^{(2)}\| I)$$

Therefore,

$$(I\| T^{(2)}\| I) = eQ/2\begin{pmatrix} I & I & 2 \\ -I & I & 0 \end{pmatrix}$$

Equation 42 now reads

$$\langle I,M'|\mathcal{H}_{el}| I,M\rangle = \left(\frac{2\pi}{5}\right)^{\frac{1}{2}} (-1)^{I-M'} \frac{eQ}{2\begin{pmatrix} I & I & 2 \\ -I & I & 0 \end{pmatrix}} V_{-\mu}^{(2)} \begin{pmatrix} I & I & 2 \\ -M & M' & \mu \end{pmatrix}$$

(43)

The operator $V^{(2)}_{-\mu}$ is in the molecule fixed frame. For a molecule with axial symmetry, this operator has the form

$$V^{(2)}_{-\mu} = -\tfrac{1}{2} \frac{\partial^2 V}{\partial z^2} Y^{(2)}_{-q} (\beta\gamma)$$

in the space fixed frame and can be replaced by (Shimizu, 1964)

$$V^{(2)}_{0} = \frac{\eta eq}{2(6)^{\frac{1}{2}}}$$

where η is the assymetry parameter of the field gradient. The other two elements of the field operator, $V^{(2)}_{\pm 1}$ and $V^{(2)}_{\pm 2}$, are equal to zero in a molecule with axial symmetry,

The theory given above applies to a case in which there is a static quadrupole interaction. In our case, we are interested in a case where the field gradient is induced, since in a tetrahedral molecule the static gradient goes to zero. This means the correlation time above, which is the time for reorientation of the molecule, does not apply but rather we must consider a correlation time for collision (if that is the process producing the gradient). However, the M-dependence of the interaction is still the same so that the overall pattern of the spectrum pattern obtained in this way would still be the same.

6. Higher Order Interaction.

The next, higher-order, non-vanishing electric interaction term, $\iota = 4$, corresponding to hexadecapole interactions, can be evaluated in the manner used above for quadrupole interactions. The fluctuating Hamiltonian for this mechanism will lead to an equation of the form

$$\langle I,M'|\mathcal{H}_H|I,M\rangle = \frac{4\pi}{9}\sum_{\mu=-4}^{4}(-1)^{\mu+I-M}\begin{pmatrix} I & I & 4 \\ -M & M' & \mu \end{pmatrix} \times (I\|T^4\|I)V_{-\mu}^{(4)}$$

Although the electric interaction corresponding to $\iota = 3$ operators is forbidden by parity considerations, account must be taken of the possibility of a magnetic octupole mechanism for relaxation. This would lead to an equation of the type

$$\langle I,M'|\mathcal{H}_{oct}|I,M\rangle = A_{oct}\begin{pmatrix} I & I & 3 \\ -M & M' & \mu \end{pmatrix}(I\|T^{(3)}\|I)$$

where A_{oct} is some constant independent of the M states of our system.

7. Application to Scalar Coupled Multiplet Spectra.

The system considered here is the 5-spin system of four F^{19} spins (I = 1/2) and a single Ge^{73} spin (I = 9/2) in the 7.76% of molecules of $Ge^{73}F_4$ in the neat liquid phase. This spin system will be observed by high resolution studies of the F^{19} spin multiplet (decet) at 56.4 and 94.1 Mhz. The F^{19} spectrum can be idealized thus:

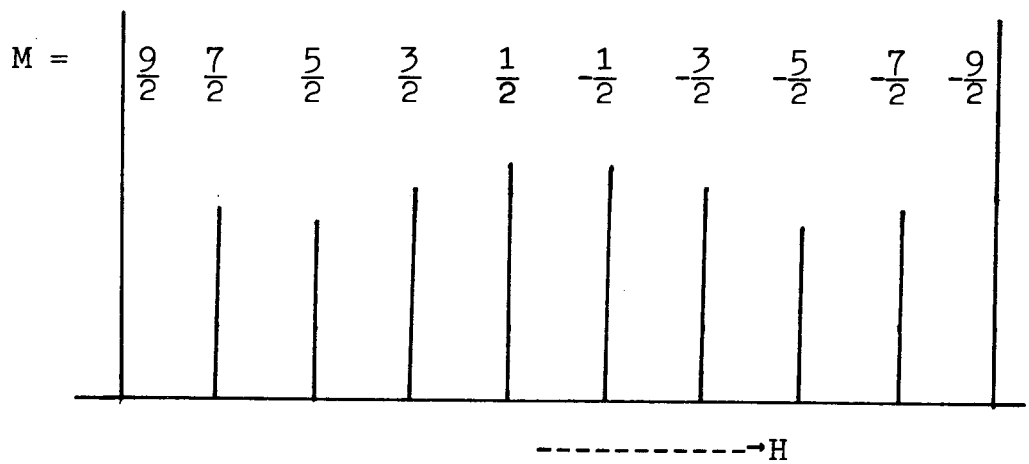

The individual F^{19} multiplet linewidths λ_M are the sum of several contributions:

a) H_o magnetic inhomogeneity effects (R^*_2 effects). Under optimum experimental conditions these can be assumed constant across the complete F^{19} decet. Time-dependent instabilities in the H_o field gradients render this assumption approximate, but in practice the field can be shimmed from time to time while recording the multiplet spectrum. (see experimental section) We assume R^*_2 constant and independent of M; i.e. it becomes a rank zero effect.

b) Natural F^{19} transverse relaxation effects, again independent of Ge^{73} M-state, (and rank zero). This can be monitored by independent measurement of F^{19} relaxation.

c) Ge^{73} relaxation transitions which cause Ge^{73} magnetization transfer from state M to state M' with probabilities $W_{MM'}$ as discussed above. These transition probabilities are M-dependent, and also rank dependent. Thus:

$$\lambda_M = R_2^* + R_2(F^{19}) + R_{2,M}(Ge^{73}) \qquad (44)$$

In the slow Ge^{73} relaxation limit, i.e.

$$R_{2,M}(Ge) << 2\pi J_{Ge-F} \qquad (45)$$

the transverse dephasing $R_{2,M}$ in the F^{19} spectrum is just the sum of all Ge transition probabilities <u>out</u> of the Ge^{73} M-state.

$$R_{2,M} = \sum_{M'} W_{MM'} \qquad (46)$$

From equations (22) and (25), the only M-dependent part of the expression for the transition probability is the Wigner 3-j symbol

$$\begin{pmatrix} I & I & \iota \\ -M & M' & \mu \end{pmatrix}$$

The rest of the terms can be represented by a scalar constant out in front of the above M-dependent matrix. This constant will vary from phenomenon to phenomenon, but will be the same for all the M states of a single relaxation mechanism. The $R_{2,M}$ is then proportional to the diagonal elements of the matrix obtained by equation (46) by summing the individual calculated $W_{MM'}$'s.

The theoretical plots that follow are line plots of what the overall peak amplitude of each line in the spectrum would be. The Ge Zeeman lines are populated according to a Boltzmann distribution, but in the so called 'high temperature' limit where the Zeeman splitting is much smaller than kT, i.e. where $\gamma_{Ge}\hbar H_o \ll kT$, (experimentally, $\gamma\hbar H_o \approx 10^{-6}kT$), the populations of the ten lines may be considered the same. This means each line has the same relative integrated area and thus the line widths can be represented by inverse height ratios. Therefore, for constant Lorentzian lineshapes, the broader the line, the shorter the peak.

Figure 2.

Rank Zero Relaxation Mechanism

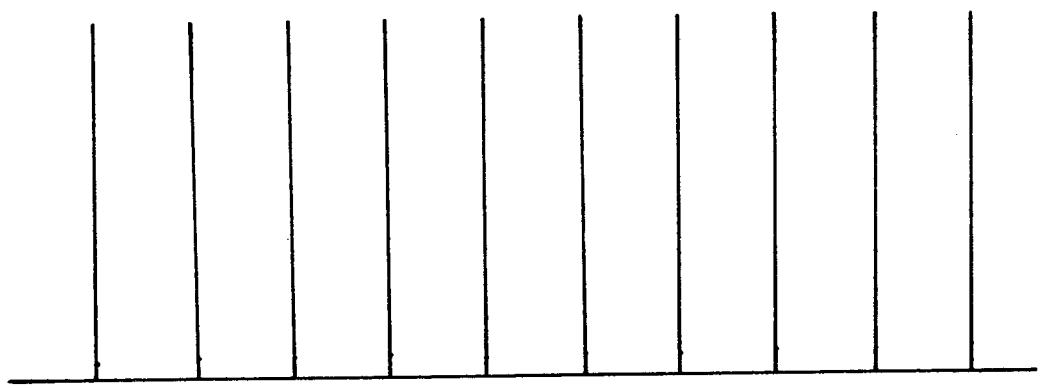

Table II

Rank One Relaxation Mechanism

$$\begin{pmatrix} I & I & 1 \\ -M & M' & \mu \end{pmatrix}^2 = \begin{pmatrix} 9/2 & 9/2 & 1 \\ -M & M' & M-M' \end{pmatrix}^2 = \frac{1}{495} \quad x$$

M \ M'	9/2	7/2	5/2	3/2	1/2	-1/2	-3/2	-5/2	-7/2	-9/2
9/2	-9	9	0	0	0	0	0	0	0	0
7/2	9	-25	16	0	0	0	0	0	0	0
5/2	0	16	-37	21	0	0	0	0	0	0
3/2	0	0	21	-45	24	0	0	0	0	0
1/2	0	0	0	24	-49	25	0	0	0	0
-1/2	0	0	0	0	25	-49	24	0	0	0
-3/2	0	0	0	0	0	24	-45	21	0	0
-5/2	0	0	0	0	0	0	21	-37	16	0
-7/2	0	0	0	0	0	0	0	16	-25	9
-9/2	0	0	0	0	0	00	0	0	9	-9

Slow relaxation limit spectral pattern (I = 9/2).

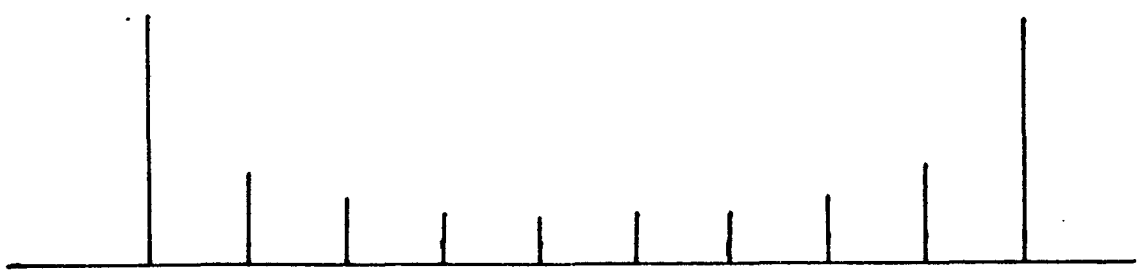

Table III

Rank Two Relaxation Mechanism

$$\begin{pmatrix} I & I & 2 \\ -M & M' & \mu \end{pmatrix}^2 = \begin{pmatrix} 9/2 & 9/2 & 2 \\ -M & M' & M-M' \end{pmatrix}^2 = \frac{1}{660} \times$$

M \ M'	9/2	7/2	5/2	3/2	1/2	-1/2	-3/2	-5/2	-7/2	-9/2
9/2	-30	24	6	0	0	0	0	0	0	0
7/2	24	-62	24	14	0	0	0	0	0	0
5/2	6	24	-65	14	21	0	0	0	0	0
3/2	0	14	14	-57	4	25	0	0	0	0
1/2	0	00	21	4	-50	0	25	0	0	0
-1/2	0	0	0	25	0	-50	4	21	0	0
-3/2	0	0	0	0	25	4	-57	14	14	0
-5/2	0	0	0	0	0	21	14	-65	24	6
-7/2	0	0	0	0	0	0	14	24	-62	24
-9/2	0	0	0	0	0	0	0	6	24	-30

Slow relaxation limit spectral pattern (I = 9/2).

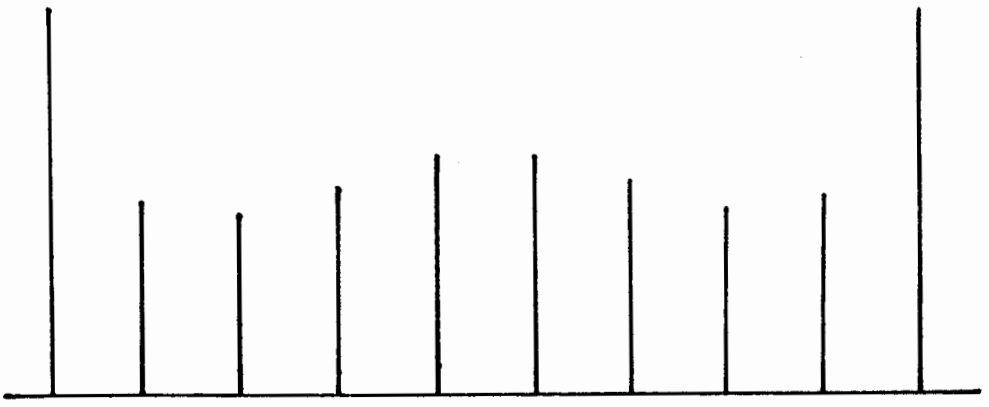

Table IV

Rank Three Relaxation Mechanism

$$\begin{pmatrix} I & I & 3 \\ -M & M' & \mu \end{pmatrix}^2 = \begin{pmatrix} 9/2 & 9/2 & 3 \\ -M & M' & M-M' \end{pmatrix}^2 = \frac{1}{60060} \quad x$$

M \ M'	9/2	7/2	5/2	3/2	1/2	-1/2	-3/2	-5/2	-7/2	-9/2
9/2	-3066	1176	1470	420	0	0	0	0	0	0
7/2	1176	-4634	588	1750	1120	0	0	0	0	0
5/2	1470	588	-4781	28	945	1750	0	0	0	0
3/2	420	1750	28	-5045	722	125	2000	0	0	0
1/2	0	1120	945	722	-5862	1200	125	1750	0	0
-1/2	0	0	1750	125	1200	-5862	722	945	1120	0
-3/2	0	0	0	2000	125	722	-5045	28	1750	0
-5/2	0	0	0	0	1750	945	28	-4781	588	1470
-7/2	0	0	0	0	0	1120	1750	588	-4434	1176
-9/2	0	0	0	0	0	0	420	1470	1176	-3066

Slow Relaxation limit spectral pattern (I = 9/2).

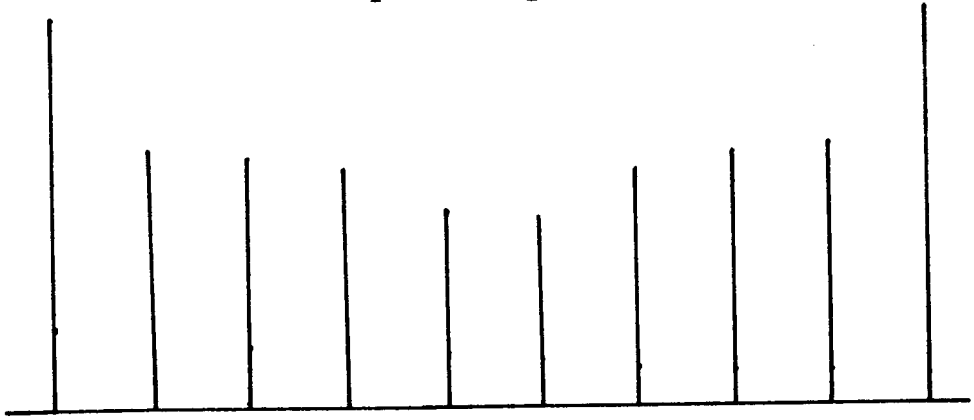

Table V

Rank Four Relaxation Mechanism

$$\begin{pmatrix} I & I & 4 \\ -M & M' & \mu \end{pmatrix}^2 = \begin{pmatrix} 9/2 & 9/2 & 4 \\ -M & M' & M-M' \end{pmatrix}^2 = \frac{1}{5148} \quad x$$

M \ M'	9/2	7/2	5/2	3/2	1/2	-1/2	-3/2	-5/2	-7/2	-9/2
9/2	-450	144	162	108	36	0	0	0	0	0
7/2	144	-418	4	42	128	100	0	0	0	0
5/2	162	4	-457	84	7	50	150	0	0	0
3/2	108	42	84	-513	54	75	0	150	0	0
1/2	36	128	7	54	-450	0	75	50	100	0
-1/2	0	100	50	75	0	-450	54	7	128	36
-3/2	0	0	150	0	75	54	-513	84	42	108
-5/2	0	0	0	150	50	7	84	-457	4	162
-7/2	0	0	0	0	100	128	42	4	-418	144
-9/2	0	0	0	0	0	36	108	162	144	-450

Slow relaxation limit spectral pattern (I = 9/2).

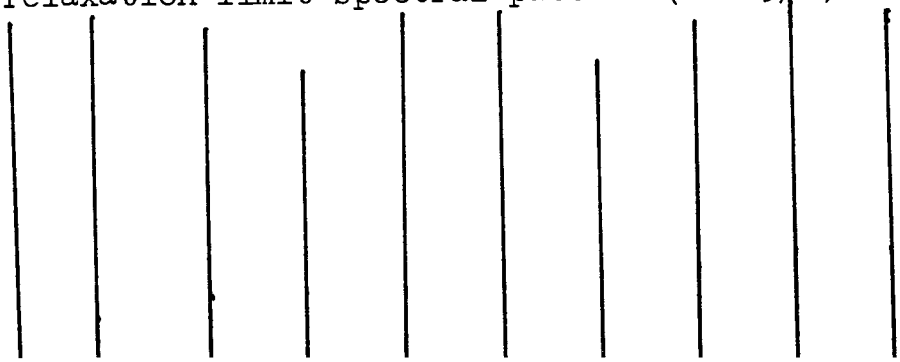

The predicted spectral patterns for each rank relaxation mechanism of a spin-9/2 nucleus in the slow relaxation limit are given below the calculated relaxation matrices. From equation (46), the widths are proportional to the diagonal matrix elements, and the plotted peak heights are inversely proportional to them. The pertinent features of the theoretical patterns are:

The rank zero spectrum has no M-dependence. Multiplet linewidths and peak heights are constant;

Rank one and rank three magnetic interactions yield somewhat similar patterns, in that the broadest components are the central ones and the sharpest are the outer ones.

Rank two interactions give a characteristic humped pattern with the sharpest components being the outer and central lines.

Rank four interactions result in a pattern very similar to rank zero, and one may anticipate experimental difficulties in distinguishing between them.

Chapter 3

Experimental

An attempt to obtain an anhydrous sample of GeF_4 (ROC/RIC, Ge-08 anhydrous 99.9% pure) was carried out in the vacuum system drawn in Figure 3. Approximately 3 gm of reagent grade NaF was placed in the two traps and the cylinder of GeF_4 was attached. The system was then evacuated, and, with the pump still on, the glass was heated to approximately 120° C and kept at this temperature for about 8 hr. After the system had cooled down to room temperature, the stopcock was closed, a liquid N_2 bath placed around trap #1 and, to prevent any GeF_4 accidently getting into the pump, a dry-ice/acetone bath was placed around trap #2. The system was then opened to the pump and the cylinder of GeF_4 opened to the system. Since the amount of sample present could not be measured by a manometer (GeF_4 reacts readily with mercury (Dennis and Laubengayer, 1927)), the quantity was approximated by eye as the white GeF_4 could be readily seen as it condensed on the walls of the trap. After sufficient sample was assumed to have come over, the cylinder was closed off and disconnected from the system. The stopcock was then closed, the cold baths removed and the system allowed to come to equilibrium at room temperature.

Figure 3

Vacuum system for obtaining GeF_4 sample.

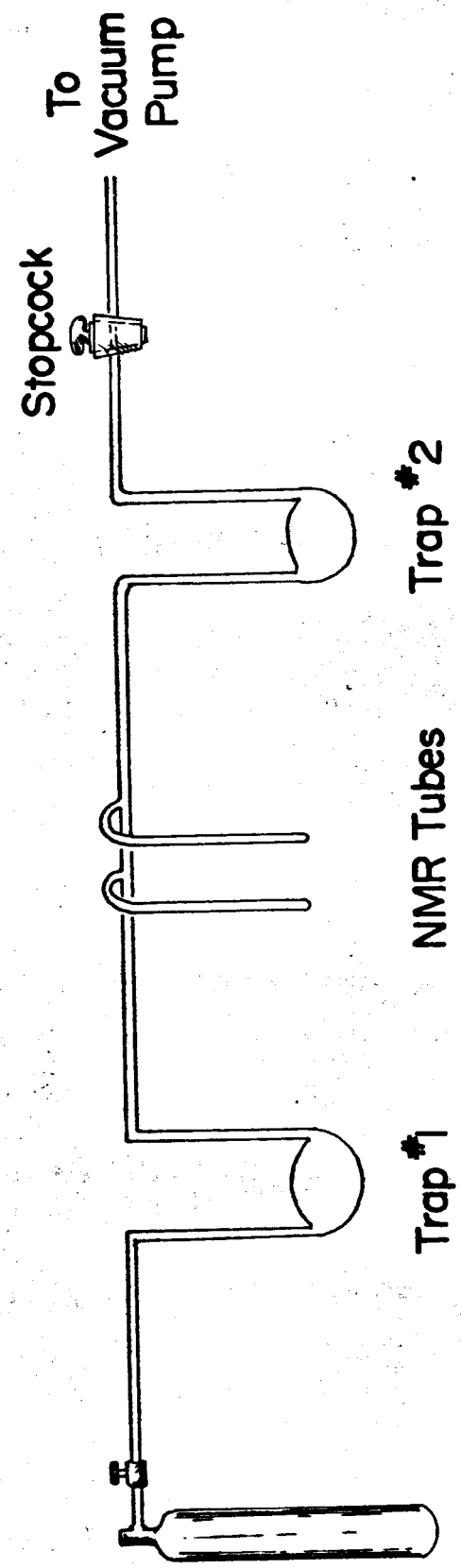

Figure 3.

After allowing the GeF_4 to remain over the NaF for several hours, the liquid N_2 bath was again placed around trap 1 in an attempt to trap all the gaseous GeF_4 in this trap. The system was pumped on once more and then the liquid N_2 trap placed around the NMR tube. No GeF_4 appeared in the NMR tube, even if the system was pumped on. This was explained when the reactions of Ge were studied. In the presence of water, GeF_4 gives an acidic solution containing GeF_6^{-2}, which readily forms a solid with NaF present (Encylopedia of Chemical Technology, 1966); (Johnson, 1952).

$$4GeF_4 + 4H_2O = 2GeO_2 + 2H_2G3F_6 + 4HF$$

$$GeF_6^{-2} + 2Na^+ = Na_2GeF_6$$

The method then used to rid the system of moisture was that given by Dennis and Laubengayer (1927). The apparatus was pumped out with a vacuum pump and heated to drive off the water from the glass surfaces. A small amount of GeF_4 was then introduced into the system which was hydrolyzed by the moisture present, the GeO_2 so produced deposited on the walls of the system and the HF pumped out. A new sample of GeF_4 was then added and by use of fractional distillations (Dennis and Laubengayer, 1927) a sealed sample of GeF_4 was obtained in the NMR

tube. The sample so obtained was kept in a dry-ice/ acetone bath to prevent decomposition of the sample.

The F^{19} spectra of GeF_4 were obtained on the fluorine mode of the Varian A56/60 spectrometer in the temperature range +36°C to -25°C. Temperatures were checked by switching to 60 Mhz, obtaining the H^1 resonance methanol shift calibration and then returning to 56.4 Mhz and scanning the spectrum. The spectra were obtained an a 1000 hz chart width at a pen speed of 0.4 cps. Saturation effects were checked by scanning the peaks at different speeds and watching for changes in amplitude of matching peaks. In this way, it was determined that a scanning speed of 0.4 cps was slow enough to prevent saturation. Homogeneity effects were checked in two ways: the instrument was 'tuned up' on the impurity lines in the spectra (which were sharper than the lines due to the Ge-bound fluorines); or else the machine was set up anew for each peak in the multiplet. GeF_4 was also run on the XL-100 Varian NMR spectrometer which became available after the bulk of this work was complete. To insure reproducibility of results, each set of peaks was scanned four times and the half-heights widths of the four peaks averaged.

T_1 measurements on GeF_4 were done on the A56/60

spectrometer (rapid adiabatic passage, Abragam, Chap. III) and on the pulse NMR spectrometer ($\pi/2$-$\pi/2$ pulse sequence).

The set of five-independent linewidth data, λ_M, at each temperature (five, since the decet was found to be symmetric about the centre) was now decomposed into a linear combination of relaxation mechanisms of ranks zero through four.

$$\lambda_M = \sum_{\Omega=0}^{4} a^{\Omega}\lambda_M^{\Omega}$$

where the λ^{Ω} patterns are given, for a given Ω rank, by the diagonal elements of the relaxation matrix in the slow relaxation limit. Here the a^{Ω} are the coefficients of the various rank interactions in the overall Ge^{73} relaxation pathway, and are to be experimentally determined.

This calculation was carried out in different ways. A Hewlett-Packard model 9100B calculator was used to solve the five simultaneous equations with five unknowns formed by the above equation. The $a^{(3)}$ (coefficient for rank three interactions) and $a^{(4)}$ (corresponding to rank four interactions) obtained in this manner as a function of temperature were highly erratic, jumping between large negative and large positive numbers, with no recognizable

continuity between them; i.e. there was no smoothly varying temperature dependence evident for rank three and rank four interactions. This we took to mean that by adding in the rank three and rank four contributions, we were attempting an unnatural fit of theoretical parameters to experimental data. This conclusion was also obtained when a least-squares fit of various combinations of the rank contributions was carried out on the IBM 360/50 computer. In this case, the rank four contribution, when added in with a sum of the rank zero and rank two contributions, came out very small comparatively or even negative. Rank three contributions on a similar fit gave predominantly zero contribution.

From these experiences it was concluded that no systematic contributions from rank three or rank four mechanisms were present in our data.

The problem then reduced to obtaining contributions from ranks zero, one and two mechanisms from the five multiplet half-patterns at each temperature. This problem is over-determined, so that a least squares fit to the coefficients $a^{(\Omega)}, \Omega = 0, 1, 2$ could be performed. However once again the derived $a^{(1)}$'s were small, erratic, non-smooth functions of temperature, forcing the conclusion that first rank contribution is negligible.

The only consistent, non-zero, non-negative contributions were calculated in the case of rank two interactions.

The final analysis is then a least squares fit to just rank zero and rank two mechanisms. The derived coefficients from this final fit are listed in Table IX.

Chapter 4

Results

Figure 4 shows the spectrum of GeF_4 at 17°C, taken on the A56/60 NMR spectrometer. It clearly shows the singlet due to the fluorine attached to zero spin germanium (Table VI) and the ten line multiplet due to fluorine attached to Ge^{73}. The coupling was measured to be 179 $\pm$ 1 hz. There are also present two bands due to decomposition of the GeF_4. These are indicated by the small arrows. Figure 5 is the same compound at -20°C run on the XL-100 NMR spectrometer. The center band has been deleted on the reproduction.

T_1 measurements on the F^{19} gave the following results:

22°C = T_1 of 9 sec.

-10°C = T_1 of 10 sec.

-20°C = T_1 of 11 sec.

Table VII lists the experimental line widths at half-height of the five peaks at the different temperatures, and Table VIII lists the line widths calculated by the computer in the least squares fit of the quadrupolar interaction to the experimental data. Table IX lists the rank zero and rank two coefficients, $a^{(0)}$ and $a^{(2)}$, calculated by the computer as a function of temperature. The plot of log $a^{(2)}$

vs $1/T°K$, shown in Figure 6, was used to measure the activation energy of the relaxation process. This was done by doing a least squares fit of the plot in Figure 6 to obtain the slope.

The rank zero contribution, $a^{(0)}$, can arise from a number of processes. The magnetic inhomogeneity gives at most a contribution of 0.3 hz. The contribution from the fluorine T_1 $(= 1/\pi T_1)$ is of the order of 0.03 hz and thus negligible. Since HF is present, it was also expected that chemical exchange processes were present in the sample. However, in the limit of this experiment, the rate of exchange should increase with temperature, a criterion not followed by the system since no systematic temperature depencence is shown by the values for $a^{(0)}$. Thus we could conclude that the effects of chemical exchange were not dominant in this case.

One possible explanation for the large $a^{(0)}$ values at low temperatures could be viscosity broadening. However, this would also affect the line width of the SiF_4 impurity peak, and this was not noticed, the SiF_4 peak showing a fairly consistent line width over the temperature range studied here. It should be noted here that although two sealed samples of GeF_4 were prepared, the data used here in the analysis was obtained from spectra run on only one

of the samples. This would then tend to rule out any broadening effects arising from impurity in the sample.

Experimental difficulties were more ways in which the large $a^{(0)}$ values could be explained. Due to the external lock on the A56/60, there is a tendency for an H_{2O}-drift with temperature. Furthermore, since the homogeneity was maximized from peak to peak, the $a^{(0)}$ cannot really be assumed a constant across the spectrum.

Probably the best reason for the $a^{(0)}$ values shown in Table IX is given by considering the effects of radiation damping, a process whose eventual result is the vanishing of the transverse magnetization (Equation 11) and thereby imposing an extra broadening on the line widths. It is a process which has been seen to have a very serious affect on the spectra produced on the XL-100 NMR spectrometer, so that it is entirely reasonable to suppose that the phenomenon is present in the A56/60, even if it is not so readily apparent in this case.

The scatter of the $a^{(2)}$ points was assumed to arise from thermal effects. Above 30°C, we observed the liquid to reflux in the tube, leading to a thermally inhomogeneous sample in the probe. Although we also did some measurements below the triple point of GeF_4 (-15°C), indicating supercooling in the sample, we also

observed a sharp freezing point, not expected in a supercooled liquid but entirely consistent with the results obtained by Dennis and Laubengayer (1927). Thus we could rule out any effects resulting from inconsistent melting points of the GeF_4 liquid in the NMR tube.

Figure 4

A56/60 Spectrum of GeF_4 at 17°C

Figure 4

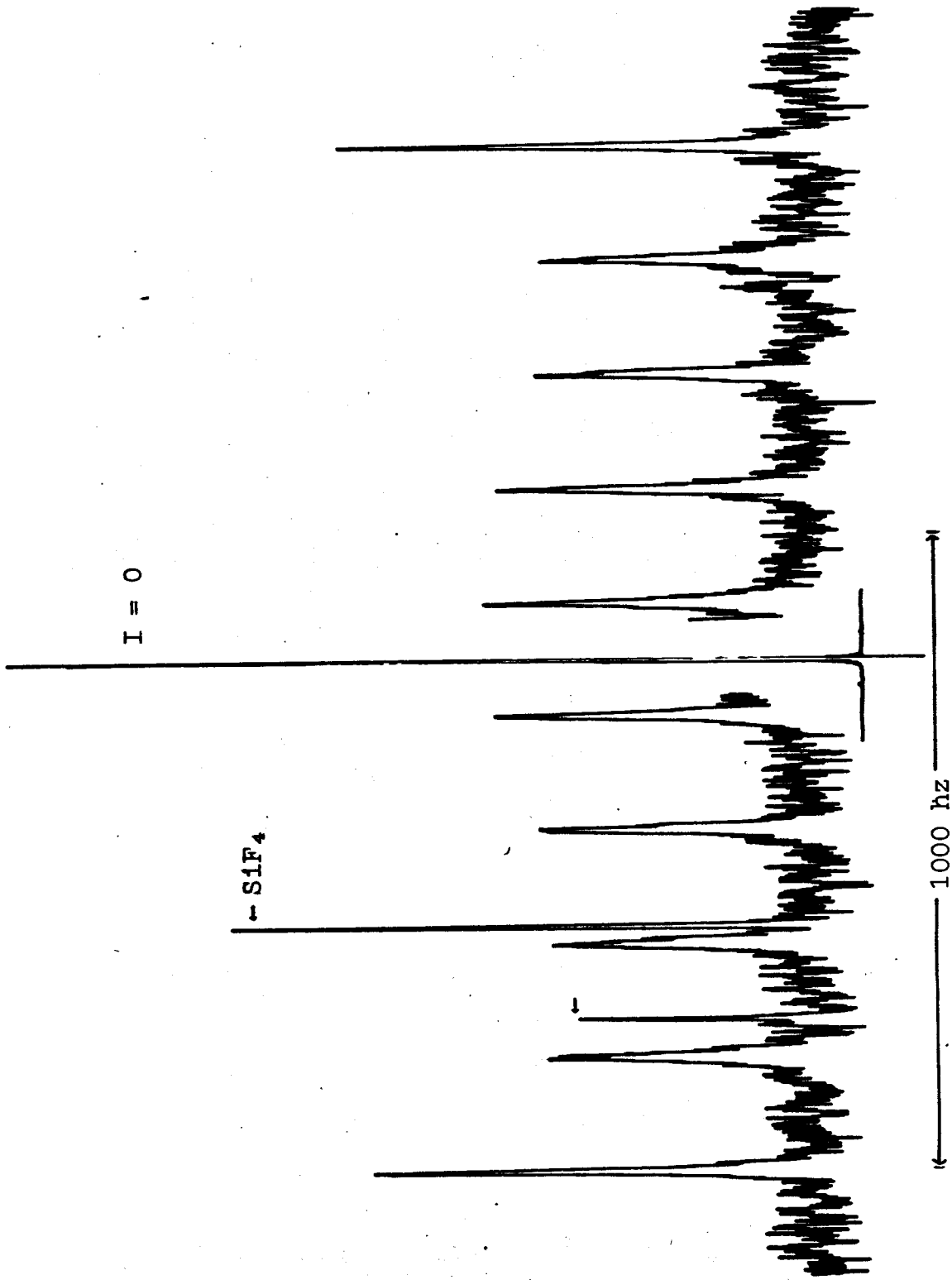

Table VI

Magnetic Properties of Ge and U Nuclei

Isotope	% Natural Abundance	Spin units of $\hbar$	μ units of $e\hbar/2$ Mc
Ge^{70}	20.52	0	
Ge^{72}	27.43	0	
Ge^{73}	7.76	9/2	-.87677
Ge^{74}	36.54	0	
Ge^{76}	7.76	0	
U^{234}	.0057	0	
U^{235}	.72	7/2	.35
U^{238}	99.27	0	
H^{1}	99.984	1/2	2.79268
F^{19}	100.	1/2	2.6273

Figure 5

XL-100 Spectrum of GeF_4 at -21°C

Large centre band has been deleted.

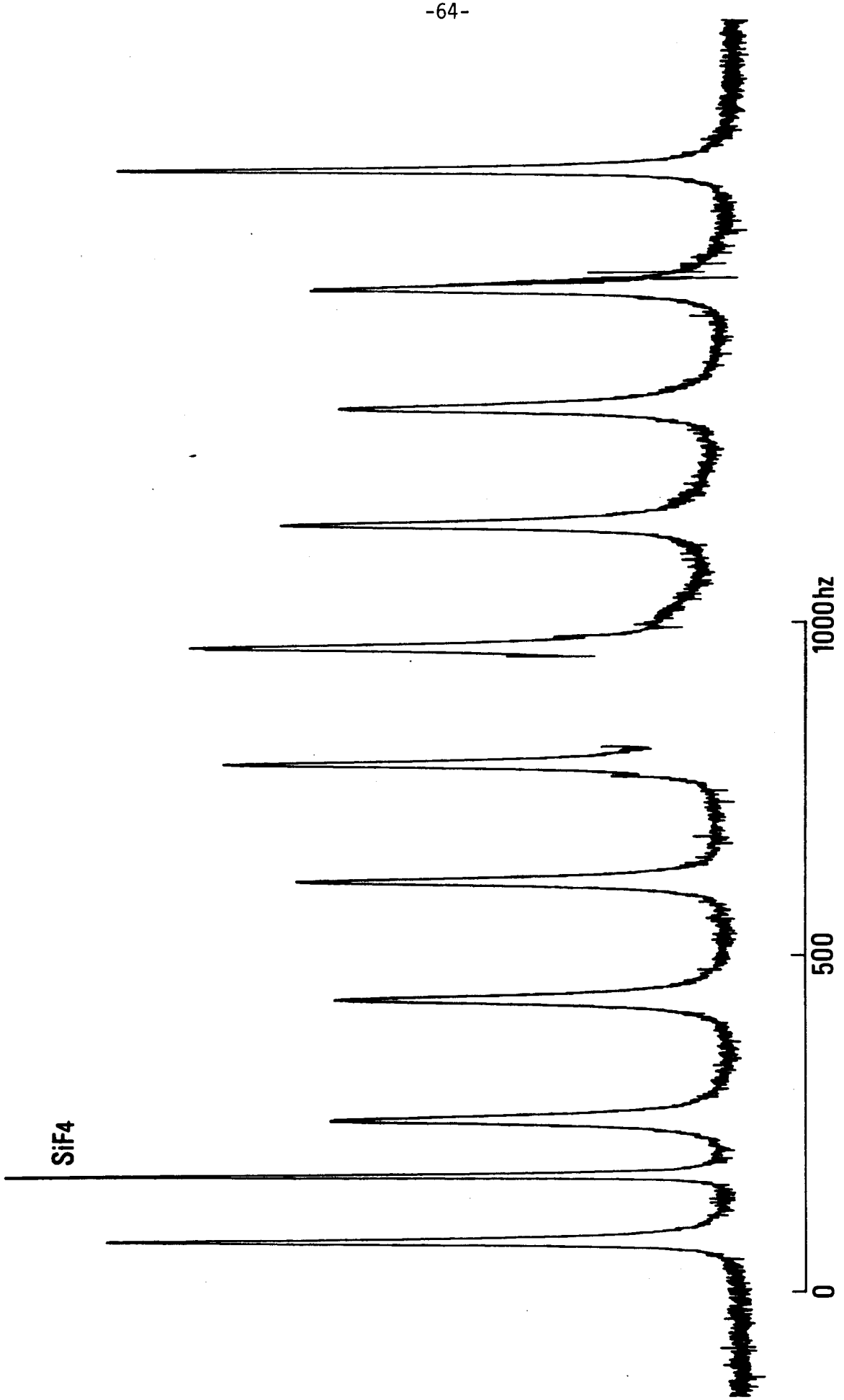
SiF4
0
500
1000hz

Table VII

Experimental Line Widths (hz)

(full width at half height)

peak Temperature	1	2	3	4	5
36°	6.0	9.2	10.2	9.2	8.0
33.5°	7.0	13.5	13.9	12.3	11.2
31°	7.0	13.0	14.5	10.5	7.5
30°	7.0	12.0	13.0	11.0	9.0
22°	8.0	13.0	13.2	11.8	10.8
17°	6.0	12.0	13.0	11.0	10.0
16°	7.0	13.5	15.0	13.0	12.0
12°	7.0	13.5	14.0	12.5	11.7
9°	8.0	14.5	15.5	14.0	12.0
-4°	9.0	15.6	16.5	15.0	14.9
-6°	9.5	16.0	17.0	15.0	12.5
-20°	12.5	22.0	24.0	22.0	18.0
-25°	9.8	18.0	19.6	17.8	17.3

Table VIII

Calculated Line Widths

(hz)

Peak Temperature	1	2	3	3	4	5
36°	6.0	9.5		9.8	9.0	8.2
33.5°	7.0	13.4		14.0	12.4	11.0
31°	5.8	12.4		13.0	11.4	9.9
30°	6.5	11.9		12.4	11.1	9.9
22°	7.9	12.8		13.2	12.0	10.9
17°	6.0	12.2		12.8	12.2	9.9
16°	7.2	14.1		14.7	13.0	11.5
12°	7.4	13.5		14.0	12.5	11.9
9°	8.0	14.7		15.4	13.7	12.2
-4°						
-6°	6.1	16.2		17.1	14.6	12.4
-20°	12.3	23.6		22.7	21.0	18.8
-25°						

Figure 6

Temperature Dependence of
a^2.

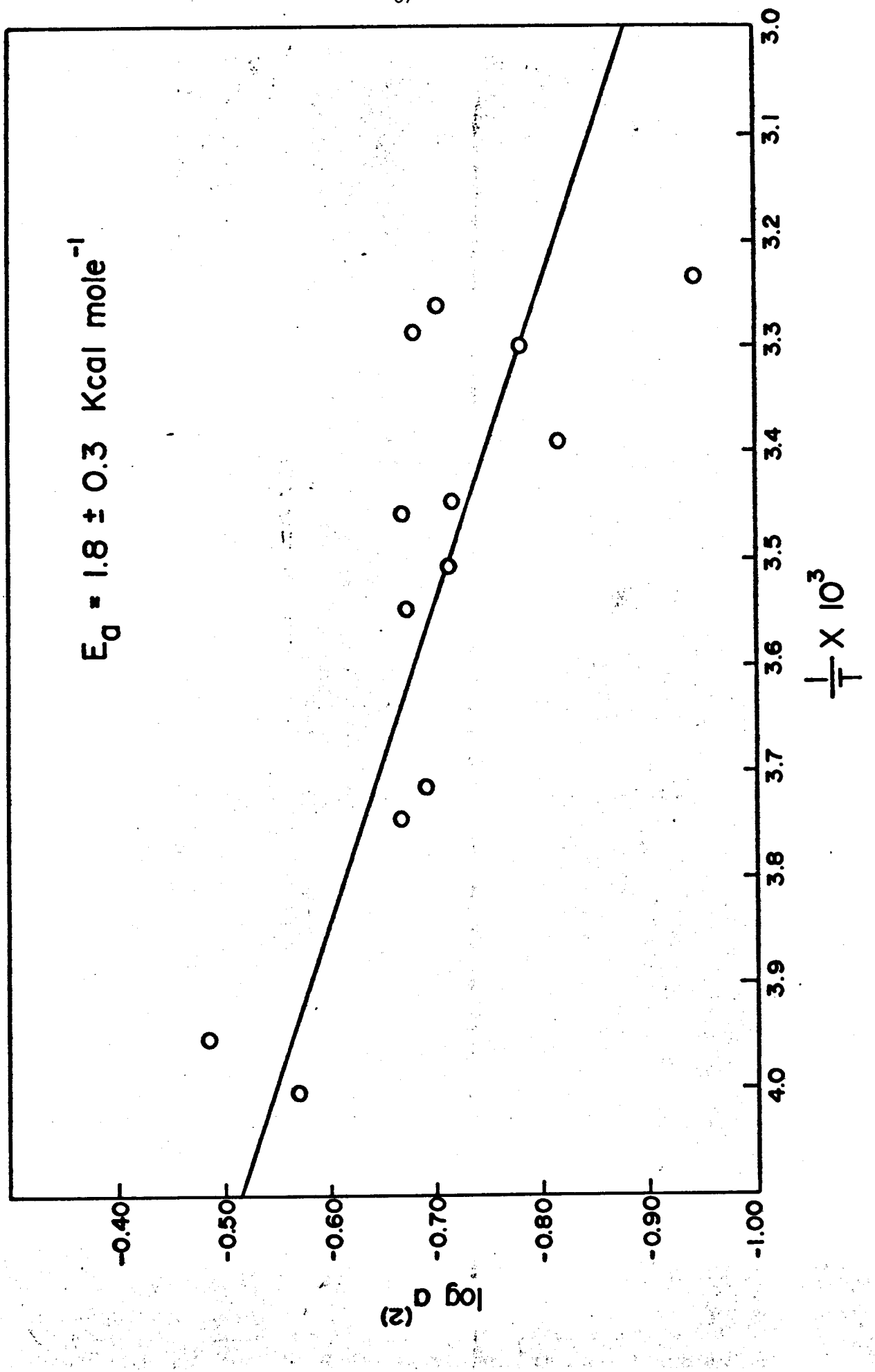
E_a = 1.8 ± 0.3 Kcal mole^{-1}
log $\sigma(\Omega)$
-0.40
-0.50
-0.60
-0.70
-0.80
-0.90
-1.00
4.0
3.9
3.8
3.7
3.6
3.5
3.4
3.3
3.2
3.1
3.0
$\frac{1}{T} \times 10^3$

Table IX

Rank Zero and Two Contributions

Temperature	$a^{(0)}$	$a^{(2)}$
36°	2.70	.11
33.5°	1.61	.20
31°	-.44	.21
30°	1.46	.17
22°	3.33	.15
17°	.21	.19
16°	.78	.22
12°	1.74	.20
9°	1.57	.21
-4°	3.30	.20
-6°	2.72	.21
-20°	2.57	.32
-25°	2.66	.27

Chapter 5

Discussion

Visual inspection of the experimental spectral pattern over all temperatures obtained here, and comparison with the theoretical patterns, shows that the dominant Ge^{73} relaxation mechanism is due to a second rank spin tensor operator. This conclusion is also borne out by the computer decomposition of the pattern, and allows one to immediately identify the relaxation pathway as predominantly due to a quadrupolar mechanism. Thus the first rank Ge^{73} interactions, comprising spin-rotation interaction, intramolecular dipole-dipole interaction (Ge^{73} to F^{19}), chemical shift anisotropy and paramagnetic impurity interactions can all be dismissed as unimportant. Of these, the σ-anisotropy is expected to vanish by symmetry, the paramagnetic impurity $\vec{I}.\vec{S}$ interaction is known to be small from the long F^{19} T_1 values (~10 sec) measured on the same sample, and the spin-rotation interaction in the rotational diffusion limit ($\tau_J << \tau_2$) would have the opposite temperature dependence to that observed here for Ge^{73}. Thus it could appear that the only first rank interaction that might contribute with the correct temperature dependence would be intramolecular dipole. However, this also may be expected to

be small by the following argument: Although a definitive study of F^{19} spin-lattice relaxation in liquid GeF_4 has not been carried out, our data indicates that T_1 is approximately independent of temperature over the range -25°C to +31°C. This may be taken as evidence of competition at F^{19} between the spin-rotation and dipolar mechanisms; i.e. the dipole mechanism does not even dominate the F^{19} relaxation. But the ratio of the dipole mechanisms at F^{19} and Ge^{73} in GeF_4 is approximately

$$\frac{R_{1\,\text{dipole}}(Ge)}{R_{1\,\text{dipole}}(F)} \approx \frac{\gamma_{Ge}^2}{\gamma_F^2} \cdot \frac{4}{3} \cdot \left(\frac{r_{F-F}}{r_{Ge-F}}\right)^6 \approx 0.04$$

with $r_{Ge-F} = 1.67\text{Å}$ and $r_{F-F} = 2.73\text{Å}$, where the small value of this ratio is due to the small value of γ_{Ge}. Thus the intramolecular dipole mechanism at Ge^{73} cannot explain the observed 8-15 hz linewidths of F^{19}.

In addition, the observed multiplet patterns do not follow those calculated for the higher rank interactions. The non-contribution of the third rank octupole to relaxation can be rationalized by noting that this is a <u>magnetic</u> interaction and would require the existence of resultant orbital or spin or rotational angular momentum fixed in the molecule. For diamagnetic

GeF_4, both $\vec{L}$ and $\vec{S}$ vanish, and the non-vanishing $\vec{J}$ contributes in first order to the (apparently small) spin-rotation interaction. The fourth rank hexadecapole interaction is electrostatic and is expected in general not to vanish to first order in a tetrahedral molecule. Unfortunately, for a spin-9/2 nucleus, the theoretical pattern for the fourth rank interaction is close to that for zero rank, and so the present data do not allow us, even in principle, to separate unequivocally these effects from H_o inhomogeneity. However, we can conclude from the spectra that the hexadecapole interaction makes at most an insignificant contribution to the Ge^{73} relaxation.

Nature of the Symmetry Distortion in GeF_4

The conclusion above that Ge^{73} in liquid GeF_4 relaxes by a quadrupole mechanism raises the question of the mechanism by which a non-vanishing electric field gradient is generated in this tetrahedral species. Four distorting mechanisms were considered.

a) Asymmetric vibrations can generate instantaneous field gradients that fluctuate at the normal mode frequency. However, the spin relaxation transition

is due only to the component of this fluctuation at the Larmor frequency. We take the fact that the vibrational spectrum (i.e. in IR or Raman spectroscopy) is sharp in condensed phases as prima facie evidence that the spectral density of this mode tends to zero at low frequencies, i.e. as evidence that there is no low frequency tail to the mode on progressing to the liquid. This observation can then be used to discard this mechanism as being responsible for the relaxation studied.

b) Centrifugal distortion in the tetrahedral GeF_4 system is different to that in the octohedral MoF_6 case discussed by Brooks (1969). Here, for rotation about a J-vector aligned along a Ge-F bond, the distortion would have components in both the angle bend and bond stretch modes; and since in general the bending force constants are smaller than those for stretching, the possibility for significant distortion exists. In addition, there is some evidence that small spherical molecules persist in free rotation in the liquid phase (Bloom, 1967), so that the rotational motion leading to distortion may not be quenched here.

However, the following simple-minded argument about the expected temperature-dependence of this

mechanism may be used to rule it out as important at the temperatures studied here. An off-axis mass-point on a classical rigid rotor experiences a centrifugal force $f = mrJ^2/I^2$ where I is the moment of inertia and J^2 (which is proportional to T, assuming equipartition of energy) is the square of the rotational angular momentum. For a non-rigid rotor, the deformation is proportional to the force, and thus proportional to the temperature. If we now assume that the electric field gradient, eq, at the centre induced by the distortion, is proportional to the distortion and note that the resultant spin relaxation is proportional to $(eq)^2$, we find that the relaxation due to this mechanism would vary as T^2. Since the temperature dependence of the correlation time τ_j for fluctuations in the J-vector is exponential, we have for the total temperature dependence

$$R_1(\text{distortion}) \propto T^2 \exp(E_a/RT)$$

where typically $E_a \approx 2$ kcals mole^{-1}. Then a trivial calculation of $d(\ln R_1)/d(1/T)$ leads to an expected apparent activation energy near 300°K of 0.4 kcal mole^{-1} for the centrifugal distortion mechanism. Since the measured activation energy is 1.8 kcal mole^{-1}, we feel

confident in discarding this mechanism as applying here.

c) Asymmetric intermolecular bonding such as fluorine-bridged polymerization is known in SbF_5 liquid, and would lead to fluctuating field gradients at the Ge metal centre. Possibilities may exist for Ge to increase its co-ordination number during collision from 4 to 5 or 6. The latter co-ordination is well-known in the hexafluoro-germanate ionic species. However, such chemical association in the liquid phase would be reflected in a number of physical properties of the liquid (for example, melting point, boiling point, specific heat, entropy of vaporization, etc.), and might be expected to become apparent by correlation of these physical properties with the other Group IVB tetrafluorides. Although in general germanium tetrafluoride does not appear to be well-characterized physically, early measurement (Thorpe, 1941) of vapour pressure, melting point and boiling point exist, and give no hint of chemical association in the liquid or solid. Thus GeF_4 is a low melting point solid (-15°C) whose melting point is quite unremarkable compared with that of CF_4 (-183°C), where no possibility for association exists. Moreover, GeF_4 exhibits no liquid range at 1 atm, its sublimation point (-37°C) being well below its triple point (-15°C).

Specific heat data is not available, nor heat of sublimation, but we can conclude that GeF_4 is auto-chemically inert, and that no significant distortion can arise from this source. This conclusion is also borne out by the very small rate of fluorine intermolecular exchange that is visible in the F^{19} NMR spectra. Such exchange would presumably follow any association or polymerization in the liquid.

d) Collisional distortion is then the only remaining mechanism that we can find to explain the observed quadrupolar relaxation. In distinction to c) above, we regard this as a purely physical process operating via dispersion forces at the time of intermolecular collision. The distortion is then related to the polarizability of the individual molecules, and thus in turn to the refractive index of the bulk phase; but again such physical data is not available.

In terms of a bimolecular collision, the physical picture is fairly clear. An instantaneous, axially symmetric field gradient is generated at the centre of a normally tetrahedral molecule by dispersion forces symmetric about the intermolecular axis. The correlation time for this mechanism is not the usual reorientation time of a molecule-fixed field gradient, but instead the time between

collisions causing appreciable distortion. This correlation time may then be expected to be related to, but not identical with, the correlation time governing intermolecular dipole-dipole interaction, and the correlation time governing translational self-diffusion of the molecules in the liquid. We may note also that the extent of collisional distortion may show a slight temperature dependence due to increase in translational energy in the centre-of-mass frame of two colliding molecules--the dependence is expected to be slight because of the steep repulsive core in most realistic two-body potentials.

It would be of some interest to examine the solvent dependence of this inferred mechanism, which may offer a sensitive test of specific intermolecular interactions. Signal-to-noise considerations ruled out such a study on the natural abundance $Ge^{73}F_4$ system, however. Such a study may be feasible with the new XL-100 spectrometer, however, using 12 mm sample tubes.

The distortion mechanism proposed here is not new. A similar, though conceptually simpler, process was used long ago by Staub (1956) to explain the pressure dependence of the spin relaxation rate of the quadrupolar Xe^{131} ($I = 3/2$) nucleus in gaseous xenon samples. In that atomic case, Staub was able to estimate the distortion due to dispersion forces from the known molar

refraction. Staub found that the strong Van der Waals forces between two atoms was enough to distort the electron cloud about the nucleus and enable an efficient quadrupole relaxation mechanism to be established. This was evidenced in the very short relaxation time of Xe^{131} ($I = 3/2$) as compared to that of Xe^{129} ($I = 1/2$). By his calculation, Staub found that the relaxation time of the system should be of the order of 10 sec., if he assumed no quadrupole relaxation. However, by assuming that there was efficient relaxation by a quadrupole mechanism, the relaxation time was calculated to be of the order of 9.6×10^{-2} sec, for which the corresponding experimental value was of the order of $2,4\text{-}2.0 \times 10^{-2}$sec.

Comparison of Ge^{73} relaxation in GeF_4 and GeH_4.

After the present study was underway, it was found that Dreeskamp and Sackmann (1966) had published a short note on Ge^{73} relaxation in liquid GeH_4 over the temperature range -30°C to -60°C. Their method was similar to ours in that they observed the coupled proton multiplet lineshape. However, in their analysis, only the higher rank (≥ 2) mechanisms were considered. A reproduction of their observed multiplet is shown below.

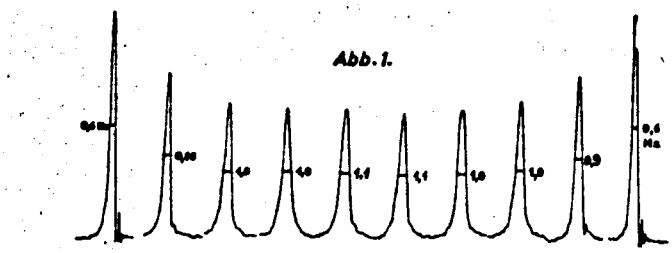

Several observations are immediate:

a) Sackmann and Dreeskamp misassigned the mechanism (as well as miscalculating several transition probabilities, and misapplying a molecule-fixed symmetry argument to transitions between space-fixed states--their argument concerning $\Delta M = \pm 2$ only, for an axially symmetric field gradient in the second rank interaction is obviously bogus, because of the necessity of transforming the spin states back to space-fixed quantization). Comparison of their spectrum with our calculated multiplet patterns indicates that in GeH_4, Ge^{73} relaxes via a <u>first</u> rank interaction. Moreover, the detailed correspondence with a rank one interaction is good; for example, after subtraction of a 0.3 hz inhomogeneity line width, their spectral line widths are (in hz)

0.3 0.55 0.7 0.7 0.8

while the rank one width sequence is

0.15 0.40 0.60 0.73 0.80

b) Sackmann and Dreeskamp state that the observed pattern is temperature independent. This allows us to infer that the Ge^{73} relaxation in GeH_4 is a competition between intramolecular dipole interaction (Ge-H) and spin-rotation interaction, both rank one interactions with opposite temperature dependence.

c) The overall Ge^{73} relaxation rate in GeH_4, as reflected in the H^1 multiplet linewidths, is slower by a factor of 20 than the corresponding rate in GeF_4, and the dominant mechanism is different. This accounts for our inability to isolate unambiguously the first rank relaxation contribution in GeF_4, which would be expected to be comparable in magnitude to that in GeH_4.

d) Even in GeH_4, where the Ge^{73} relaxation is slow (with resulting linewidths comparable to the inhomogeneity width) there is no clear evidence for the hexadecapole interaction.

It is of some interest to enquire as to the reason for the very different behaviour of the Ge^{73} spin in these two closely related systems. We may assume that the first rank (magnetic dipole) interactions are comparable in the two cases. The difference between the two systems is then that, compared to the magnitude of the first rank mechanism, the quadrupole mechanism is negligibly

small in GeH_4, and dominantly large by an order of magnitude or more in GeF_4. In terms of the mechanism proposed above, with a given collisional correlation time, this implies that the field gradient at Ge^{73} by collisional distortion in GeF_4 is at least an order of magnitude larger than that in GeH_4. Such an effect can be rationalized by noting that the major valence electron (i.e. polarizable) charge density lies outside the ligand radius in GeF_4, but inside it in GeH_4. Hence, viewed from an impacting molecule, GeF_4 is more distortable than GeH_4; in the terminology of thermodynamicists, GeH_4 would be expected to behave as a hard sphere, GeF_4 as a soft one.

The latter description yields yet another picture in the collisional time domain. The distortion fluctuation for a hard sphere comprises a series of positive and negative spikes with a repetition frequency near the collisional correlation time, so that the corresponding spectral density $J(\omega)$ is localized to a band near and above the collision frequency. $J(\omega_o)$ at the Larmor frequency may be expected to be small, so that the cross section for induced quadrupolar relaxation is small. On the other hand, the distortion fluctuation for a soft sphere may be pictured as smoothly varying function with a well-behaved correlation function and a white spectral density leading to an observable relaxation cross section.

Chapter 6

Conclusions

Ge^{73} relaxation by a quadrupolar effect seemed to account for the majority of the scalar-coupled F^{19} line widths obtained in the high resolution F^{19} spectrum of the neat liquid GeF_4, within experimental error. The static field gradient being zero for a spherically symmetrical molecule meant we had to look for some way an instantaneous field gradient could be produced at the nucleus. The mechanisms we had considered as possibilities for producing such a field gradient were:

a) asymmetric vibration

b) centrifugal distortion

c) asymmetric intermolecular bonding

d) collisional distortion

The first mechanism was discarded after noticing that there would be no low frequency tail to the vibrational mode, as was evident by the sharp, condensed phase IR (or Raman) spectrum (Woltz and Nielsen, 1952). Centrifugal distortion was ruled out by the smallness of the possible bond distortion and by a predicted temperature dependence that is much too small. No noticeable discrepancies appeared in a comparison of the physical properties of GeF_4 and the other Group IVB tetrafluorides. This meant there probably was no asymmetric intermolecular bonding

of GeF_4 molecules in the liquid. We were then left with collisional distortion as the mechanism giving rise to the second rank interaction we saw in the spectra of GeF_4, a mechanism not unknown as giving rise to quadrupole interactions, since Staub (1956) had already explained the short relaxation time of Xe^{131} ($I = 3/2$) by this method.

That we were really seeing the effects of a second rank interaction can be emphasized strongly after we compared our GeF_4 system with the GeH_4 system studied by Dreeskamp and Sackmann (1966). From a study of their spectrum, we came to the conclusion that the GeH_4 system was relaxing by a rank one interaction predominantly, and not by a rank two ($\Delta M = \pm 2$ only transitions) interaction as stated by Dreeskamp. This discrepancy in the relaxation mechanisms of the two systems was then explained in the light of the different physical pictures of the systems--GeF_4 with its major valence electron charge density lying outside the ligand radius could be regarded as a soft sphere (easily distorted) whereas GeH_4 was considered to be a hard sphere since its charge density lay largely within the circle of the ligands.

The spectrum of GeH_4 was then used to explain the relaxation mechanisms of our GeF_4 system. From a look

at the spectrum, the size of the rank one contributions to the line widths could be at the most in the range of 0.3 to 0.8 hz, and thus a negligible contribution to the line widths we saw, which were in the range 6 to 15 hz. More to the point, a comparison of the two spectra allowed us to say something about the hexadecapole interaction. In the spectrum of GeH_4, no evidence was found for the presence of rank four interactions. If there was a possibility of rank four interactions in the Ge^{73} relaxation processes, it would be seen more clearly in the sharp lines of the GeH_4 spectrum, since they would be more sensitive to changes in peak amplitudes, since they were so sharp. Therefore, since we expect $\partial^4 V / \partial z^4$ to be comparable in both systems, if the rank four interaction did not show up in the GeH_4 system, we felt we could rule it out as a predominant relaxation mechanism in the GeF_4 case.

Chapter 7

Tetramethyl Germanium $Ge(CH_3)_4$

The work that was done on GeF_4 was also attempted on a sample of $Ge(CH_3)_4$ (Alfa Inorganics). Figure 7 shows a typical spectrum of the neat liquid at room temperature obtained on the proton mode of the Varian A56/60 NMR spectrometer. Since our analysis depended on the lines being first order Lorentzian, the overlap of the lines in the spectrum ruled out the possibility of analyzing the lines by straight-forward measuring of line widths. An attempt was made to fit Lorentzian lines to the outer peaks using a curve resolver, but the results were not useable.

Uranium Hexafluoride UF_6

To purify UF_6 (Varlacoid Chemical Company, E-46152), apparatus similar to Figure 3 was used, again with NaF in the apparatus. After the system was baked out and cooled, UF_6 was introduced into the system. Upon contact with the NaF, the UF_6 formed a yellow coating on the surface of the NaF. After the system had equilibrated to room temperature, the system was pumped out, and a new portion of UF_6 introduced into the system. The sample was then transferred from trap 1 to the NMR sample tube and sealed off. The sample was yellow

Figure 7

A56/60 Spectrum of $Ge(CH_3)_4$ at Rm. Tp.

$J_{Ge^{73}-H^1}$ = 3 hz

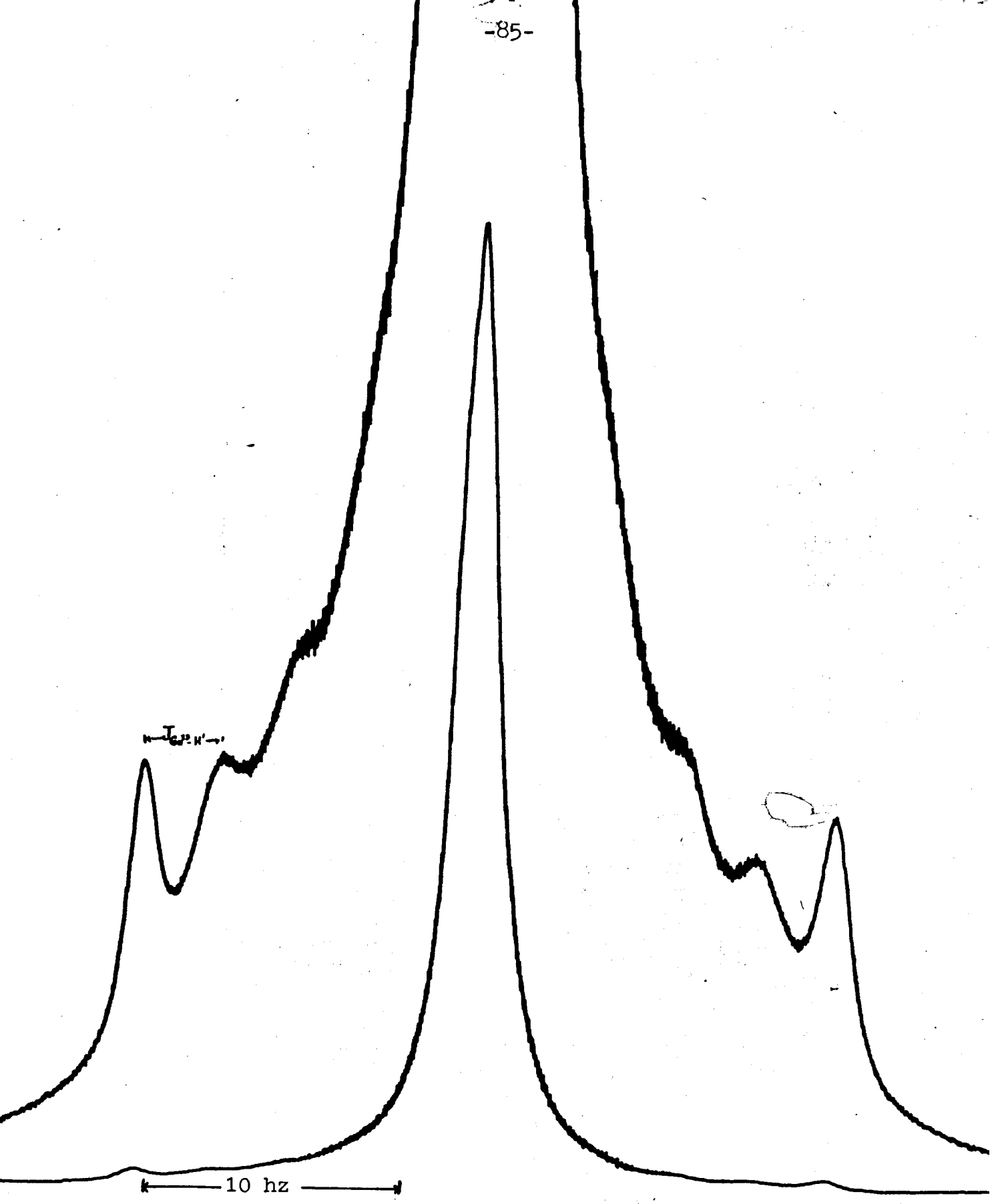

Figure 7

Germanium Tetramethyl

in color and a solid at room temperature, becoming a liquid only after being heated above 75°C. A sample was also prepared without the use of NaF but again the solid was yellow in color.

In a system of small amounts of water or HF and UF_6, a catalytic decomposition cycle starts with the silica in the glass.

$$2UF_6 + 2H_2O = 2UOF_4 + 4HF$$
$$4HF + SiO_2 = 2H_2O + SiF_4$$

The HF and SiF_4 so produced could be precipitated by the use of an alkali fluoride such as NaF.

$$NaF + HF = NaF.HF$$
$$2NaF + SiF_4 = Na_2SiF_6$$

(Grosse, 1950)

Ruff and Heinzelmann (1911) found that in the presence of NaF or KF, yellow compounds were formed between UF_6 and the alkali metal fluorides. These probably have the form UO_2F_2. Grosse (1950), however, found that these reactions stopped when the HF present was all complexed. In this way, the alkali metal fluorides could be used to stop the cycles above.

What we then did was pass the UF_6 through a column

made of anhydrous granular KF layered with glass wool (Figure 8). This presented maximum area to the UF_6 and the glass wool prevented the KF from lumping together enough to seal off the tube. In this manner a white sample of UF_6 solid was obtained in the NMR tube.

When the spectrum of UF_6 was obtained at 56.4 Mhz on the A56/60 Varian NMR spectrometer, the peaks came out as 'emission' peaks; i.e. the peaks came out 'upside down'. However, when a Schomandl ND30M external frequency synthesizer was used to modify the 21 khz modulation of the spectrometer, a small dispersion mode signal was found a very long distance upfield from the original band we had looked at. With the oscillating crystal in the NMR operating at 21 khz, we could look for sidebands every 21 khz. The small dispersion signal agreed with this so then we looked for an absortion mode signal at 42 khz from the main peak. This was not found due to the fact that the machine had cut-off filters after a specific region. The chemical shift of UF_6 was then calculated on the basis that the absorption band should come 42 khz upfield from the band we saw. This we found to be 736 ppm relative to $CFCl_3$, which is in agreement to the value given by Pople, Schneider, and Bernstein (p. 319). They give the

Figure 8

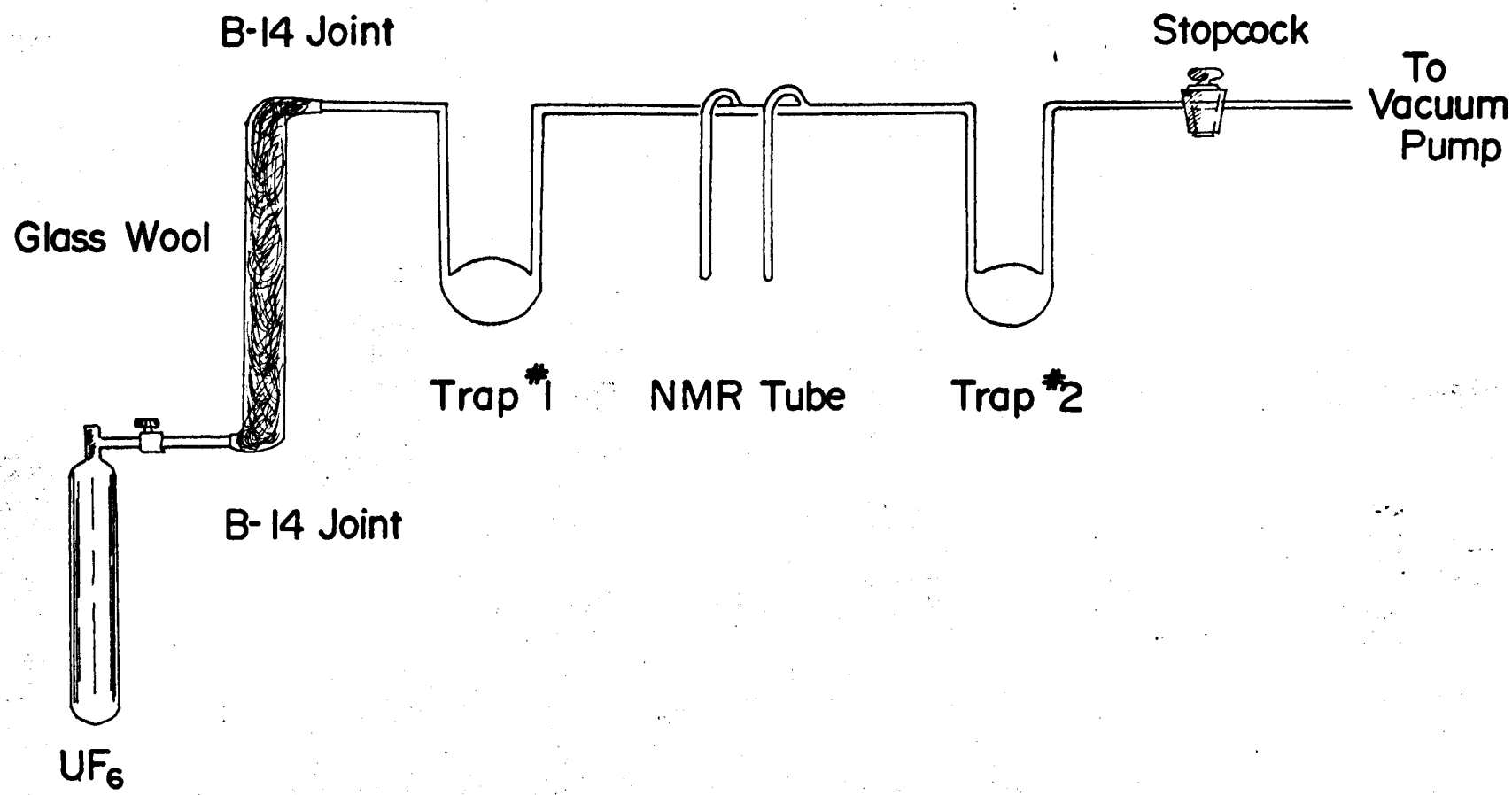
B-14 Joint
Stopcock
To Vacuum Pump
Glass Wool
Trap #1
NMR Tube
Trap #2
B-14 Joint
UF_6

value of 744 ppm. Since very little else absorbs up in this region (Figure 9) we assumed this actually was the spectrum of UF_6.

What we wanted to see was an effect similar to that found in the GeF_4 system. However, the spectrum showed no splitting. This was due either to efficient chemical exchange relaxation pathways (because of the HF present) or else the natural abundance of the quadrupole isotope U^{235} (I = 7/2) was too small for the electronics of the NMR spectrometer to detect. This could well be the case since the spectrometer had to operate at the limits of its capabilities in order for us to get usable GeF_4 spectra.

Figure 9

Some Representative F^{19} Chemical Shifts.

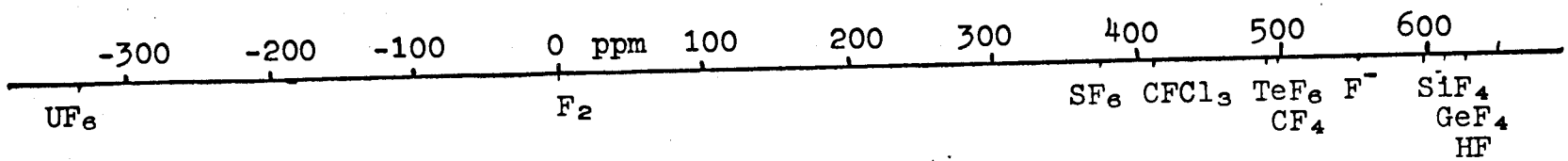

Appendix

The 3-j symbols.

The 3-j symboss defined in the main section of this thesis are listed in the book by Rotenburg, Bivins, Metropolis and Wooten as the squares of the 3-j symbols rather than as the symbols themselves since the squares of these symbols are rational fractions. The values are listed as the powers of the prime factors, the first eight of which are 2, 3, 5, 7, 11, 13, 17, 19, and are listed in increasing order with the smallest prime at the left. For Example:

$$20 = 2 \times 2 \times 5$$

$$20 = 2^2 \times 3^0 \times 5^1$$

The value listed would then be 201.

If the number is a fraction, the negative exponent is underlined.

$$\frac{12}{49} = 2^2 \times 3^1 \times 5^0 \times 7^{-2}$$

The value listed would then be 210$\underline{2}$.

The 3-j symbols used in this work are listed on the following pages.

I	I	ι	M'	M	μ	$\begin{pmatrix} I & I & \iota \\ M' & M & \mu \end{pmatrix}^2$
						2357,11
9/2	9/2	1	9/2	7/2	1	0010,1
9/2	9/2	1	7/2	5/2	1	4210,1
9/2	9/2	1	5/2	3/2	1	0111,1
9/2	9/2	1	3/2	1/2	1	3110,1
9/2	9/2	1	1/2	-1/2	1	0210,1
9/2	9/2	2	9/2	7/2	1	1010,1
9/2	9/2	2	7/2	5/2	1	1010,1
9/2	9/2	2	5/2	3/2	1	1111,1
9/2	9/2	2	3/2	1/2	1	0110,1
9/2	9/2	2	1/2	-1/2	1	0
9/2	9/2	2	9/2	5/2	2	1010,1
9/2	9/2	2	7/2	3/2	2	1111,1
9/2	9/2	2	5/2	1/2	2	2011,1
9/2	9/2	2	3/2	-1/2	2	2110,1
9/2	9/2	2	1/2	-3/2	2	2110,1
9/2	9/2	3	9/2	7/2	1	1011,11
9/2	9/2	3	7/2	5/2	1	0011,11
9/2	9/2	3	5/2	3/2	1	0110,11
9/2	9/2	3	3/2	1/2	1	1111,1102
9/2	9/2	3	1/2	-1/2	1	2011,11
9/2	9/2	3	9/2	5/2	2	1001,11
9/2	9/2	3	7/2	3/2	2	1120,11

9/2	9/2	3	5/2	1/2	2	2200,11
9/2	9/2	3	3/2	-1/2	2	2121,11
9/2	9/2	3	1/2	-3/2	2	2121,11
9/2	9/2	3	9/2	3/2	3	0000,11
9/2	9/2	3	7/2	1/2	3	3100,11
9/2	9/2	3	5/2	-1/2	3	1120,11
9/2	9/2	3	3/2	-3/2	3	2121,11
9/2	9/2	3	1/2	-5/2	3	1120,11
9/2	9/2	4	9/2	7/2	1	2000,11
9/2	9/2	4	7/2	5/2	1	0200,11
9/2	9/2	4	5/2	3/2	1	0101,11
9/2	9/2	4	3/2	1/2	1	1100,11
9/2	9/2	4	1/2	-1/2	1	0
9/2	9/2	4	9/2	5/2	2	1200,11
9/2	9/2	4	7/2	3/2	2	1101,11
9/2	9/2	4	5/2	1/2	2	2201,11
9/2	9/2	4	3/2	-1/2	2	2120,11
9/2	9/2	4	1/2	-3/2	2	2120,11
9/2	9/2	4	9/2	3/2	3	0100,11
9/2	9/2	4	7/2	1/2	3	5200,11
9/2	9/2	4	5/2	-1/2	3	1220,11
9/2	9/2	4	3/2	-3/2	3	0
9/2	9/2	4	1/2	-5/2	3	1220,11

9/2	9/2	4	9/2	1/2	4	0000,11
9/2	9/2	4	7/2	-1/2	4	0220,11
9/2	9/2	4	5/2	-3/2	4	1120,11
9/2	9/2	4	3/2	-5/2	4	1120,11
9/2	9/2	4	1/2	-7/2	4	0220,11

Stereochemistry of GeF_4

The analysis given in the thesis text was based on the assumption that the GeF_4 molecule is of tetrahedral symmetry. Caunt, Mackle and Sutton (1951) carried out electron diffraction measurements on germanium tetrafluoride gas and found no evidence for deviations from tetrahedral symmetry in their results. Furthermore, the IR and Raman work done on this molecule by Caunt, Short, and Woodward (1952) and by Woltz and Nielsen (1952) showed no evidence for distortion from the tetrahedral structure assumed for GeF_4. Thus we felt confident that our initial assumtion was not unsound.

A weaker argument for symmetry is given by the strong, unsplit center band of the spectrum due to the fluorines bonded to the zpin zero germanium isotopes. This shows either that the molecule must belong to one of the groups T_d, or D_{4h} or C_{4v}; or else that there is rapid intramolecular exchange in the system. This is not really a compelling argument since no evidence would show up in the rapid time scale the relaxation processes. occur in.

A more general argument for tetrahedral symmetry is given by Cotton and Wilkinson (1962). With regards to the stereochemistry of the Group IV compounds, they state:

> "With the exception of a few compounds of the heavier elements, such as bisthiourealead(II) chloride, in which the lead atoms are seven co-ordinate, and the $SnCl_5^-$ ion, the normal coordination numbers in this group are 4 and 6 and the respective geometries are tetrahedral and octahedral".

Freezing Point of GeF_4

Some of the NMR spectra used in this work were obtained below the triple point (-15°C) of GeF_4. Since we clearly still had a liquid in the NMR tube at temperatures down to -25°C, the sample must have supercooled. This would then imply a random freezing point, since this is a feature of supercooled liquids. This we did not observe. Instead we observed a sharp freezing point at -25°C. This phenomenon had already been noted by Dennis and Laubengayer (1927): "It supercools readily and its temperature can be carried 10° or more below its freezing point although the tube is constantly tapped". They quoted a solidifying point of -25.7°C.

Bibliography

Abragam, A. 1961. 'The Principles of Nuclear Magnetism', (Oxford University Press, London), Chapter II.

---------- 1961. P. 45.

---------- 1961. P. 268.

---------- 1961. Chapter VIII, Section IIc.

---------- 1961. P. 279.

---------- 1961. P. 299.

---------- 1961. P. 461.

---------- 1961. Chapter VI, Section I.

---------- 1961. P. 161.

Benz, H. P., Bauder, A., and Gunthard, Hs. H. 1966. J. Mol. Spect. 21 156.

Bloembergen, N., Purcell, E., and Pound, R. 1948. Phys. Rev. 73 679.

Bloom, M., and Sandhu, H. S. 1962. Can. J. Phys. 40 289.

Bloom, M., Bridges, F., and Hardy, W. 1967. Can. J. Phys. 45 3533.

Bloom, M., and DeWit, G. A. 1969. Can. J. Phys. 47 1195.

Brooks, S. A. 1969. M. Sc. Thesis, Simon Fraser University, Burnaby, B. C.

Carrington, A., and McLachlan, A. D. 1967. 'Introduction to Magnetic Resonance', (Harper and Row).

---------- 1967. P. 176.

---------- 1967. P. 177.

Casimir, H. B. G. 1936. 'On the Interaction Between Atomic Nuclei and Electrons', (Teyler's Genootschap, Haarlem).

Caunt, A. D., Mackle, H., and Sutton, L. E. 1951. Trans. Faraday Soc. 47 943.

Caunt, A. D., Short, L. N., and Woodward, L. A. 1952. Trans. Faraday Soc. 48 873.

Cotton, A. F., and Wilkinson, G. 1962. 'Advanced Inorganic Chemistry'. (John Wiley and Sons), P. 350.

Dennis, L. M., and Laubengayer, A. W. 1927. Z. Physik. Chem. 130 520.

Dreeskamp, H., and Sackmann, E. 1966. Z. Naturforschg. 21 852.

Edmonds, A. R. 1957. 'Angular Momentum in Quantum Mechanics', (Princeton University Press, Princeton), P. 109.

---------- 1957. P. 75.

Encyclopedia of Chemical Technology, 1966. (interscience Publishers), Vol. 9, P. 585.

Green, D. K., and Powles, J. G. 1965. Proc. Phys. Soc. 85 87.

Grosse, A. V. 1950. U. S. Patent, 1,533,316.

Hubbard, P. S. 1963. Phys. Rev. 131 1155.

Huntress, W. T. 1968. J. Chem. Phys. 48 3524.

Huntress, W. T. 1970. 'Advances in Magnetic Resonances' J. S. Waugh, Ed., (Academic Press), Vol. 4, P. 3.

Johnson, O. H. 1952. Chem. Rev. 51 431.

Mahler, R. J. 1966. Phys. Rev. 152 325.

Matthias, E., Schneider, W., and Steffen, R. M. 1962. Phys. Rev. 125 261.

Ozier, I., Yi, P., and Anderson, C. H. 1968. Phys. Rev. 165 92.

Pople, J., Schneider, W., and Bernstein, H. 1959. 'High Resolution Nuclear Magnetic Resonance', (McGraw and Hill).

Pound, R. V. 1950. Phys. Rev. 79 685.

Ruff. O., and Heinzelm nn, R. 1911. Z. fur Anorg. Chemie 72 65.

Rigny, P., and Virlet, J. 1967. J. Chem. Phys. 47 4645.

Rose, M. E. 1957. 'Elementary Theory of Angular Momentum', (J. Wiley and Sons), Chapter III.

---------- 1957. P. 79.

---------- 1957. Chapter V.

---------- 1957. P. 92.

Rotenberg, M., Bivins, R., Metropolis, N., and Wooten, K., Jr. 1959. 'The 3-j and 6-j Symbols. (The Technology Press, Cambridge, Massachusetts).

Shimizu, H. 1962. J. Chem. Phys. 37 765.

Shimizu, H. 1964. J. Chem. Phys. 40 754.

Staub, H. H., Brun, E., Oeser, J., and Telschow, C. G. 1954. Phys. Rev. 93 904.

Staub, H. H. 1956. Helv. Physica Acta 29 246.

Tinkham, M. 1964. 'Group Theory and Quantum Mechanics'. (McGraw and Hill, New York).

Thorpe, J., and Whitely, M. 1941. 'Thorpe's Dictionary of Applied Chemistry', 4th Ed., Vol. V, P. 522.

Woltz, P. J. H., and Nielsen, A. H. 1952. J. Chem. Phys. 20 307.